Accepted Manuscript

Carbonic anhydrase inhibitors: Design, synthesis and structural characterization of new heteroaryl-*N*-carbonylbenzenesulfonamides targeting druggable human carbonic anhydrase isoforms

Maria Rosa Buemi, Laura De Luca, Stefania Ferro, Elvira Bruno, Mariangela Ceruso, Claudiu T. Supuran, Klára Pospíšilová, Jiří Brynda, Pavlína Řezáčová, Rosaria Gitto, PhD, Associate professor on Medicinal Chemistry

PII: S0223-5234(15)30181-1

DOI: 10.1016/j.ejmech.2015.07.049

Reference: EJMECH 8033

To appear in: *European Journal of Medicinal Chemistry*

Received Date: 19 June 2015

Revised Date: 28 July 2015

Accepted Date: 30 July 2015

Please cite this article as: M.R. Buemi, L. De Luca, S. Ferro, E. Bruno, M. Ceruso, C.T. Supuran, K. Pospíšilová, J. Brynda, P. Řezáčová, R. Gitto, Carbonic anhydrase inhibitors: Design, synthesis and structural characterization of new heteroaryl-*N*-carbonylbenzenesulfonamides targeting druggable human carbonic anhydrase isoforms, *European Journal of Medicinal Chemistry* (2015), doi: 10.1016/j.ejmech.2015.07.049.

Graphical Abstract

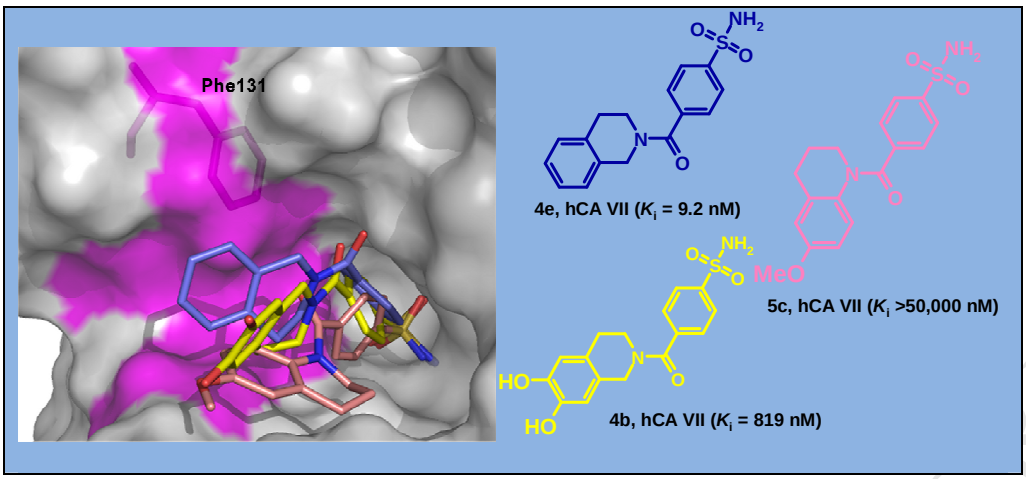

Carbonic anhydrase inhibitors: Design, synthesis and structural characterization of new heteroaryl-*N*-carbonylbenzenesulfonamides targeting druggable human carbonic anhydrase isoforms

Maria Rosa Buemi,[a] Laura De Luca,[a] Stefania Ferro,[a] Elvira Bruno,[a] Mariangela Ceruso,[b] Claudiu T. Supuran,[b] Klára Pospíšilová,[c] Jiří Brynda,[c,d] Pavlína Řezáčová,[c,d] and Rosaria Gitto[a,]*

[a]Dipartimento Scienze del Farmaco e dei Prodotti per la salute, Università degli Studi di Messina, Viale Annunziata, I-98168 Messina, Italy
[b]Neurofarba Department, Section of Pharmaceutical and Nutraceutical Sciences, Università degli Studi di Firenze, Sesto Fiorentino (Florence) , Via U. Schiff 6, 50019 Sesto Fiorentino (Florence), Italy.
[c]Institute of Molecular Genetics, ASCR, v.v.i., Vídeňská 1083, Prague 4, 14220, Czech Republic;
[d]Institute of Organic Chemistry and Biochemistry, ASCR, v.v.i., Flemingovo nám. 2, Prague 6, 16610, Czech Republic

Corresponding author: Rosaria Gitto, PhD, Associate professor on Medicinal Chemistry, Dipartimento Scienze del Farmaco e dei Prodotti per la salute, Università degli Studi di Messina, Viale Annunziata, I-98168 Messina, Italy
Tel 00390906766413, Fax 00390906766404, e-mail: rgitto@unime.it

Abstract. A set of heteroaryl-*N*-carbonylbenzenesulfonamides has been designed, synthesized, and screened as inhibitors of human carbonic anhydrases (hCAs). The new sulfonamide derivatives were tested against hCA I, hCA II, hCA VII, hCA IX, and hCA XII isoforms using acetazolamide (**AAZ**, **1)** and topiramate (**TPM, 2**) as reference compounds. Six compounds were low nanomolar inhibitors of tumor-associated hCA IX isoform (K_i values <10 nM); among them we identified three arylsulfonamides showing unexpected inefficacy over brain distributed hCA VII isoform (hCA IX/ hCAVII selectivity ratio > 1,500 for compound **5c**). Thus, these compounds can offer the opportunity to highlight the interactions preventing the inhibition of hCA VII mainly expressed in central nervous system. Thereby, we used structural and computational techniques to study in depth the interaction with hCAs. In an effort to confirm the inhibitory action we determined crystal structures of five selected heteroaryl-*N*-carbonylbenzenesulfonamides (**4a**, **4b**, **4e**, **5c**, and **5e)** in complex with hCA II. Moreover, to explore the lack of inhibitory effects of selected compounds (*e.g.* **4b** and **5c**) we also performed docking studies into hCA VII catalytic site.

Keywords: human carbonic anhydrase; isoquinoline; quinoline; X-ray; molecular docking

Abbreviations: acetazolamide (AAZ); carbonic anhydrases (CAs); N,N,N′,N′-tetramethyl-O-(1*H*-benzotriazol-1-yl)uranium hexafluorophosphate (HBTU); topiramate (TMP).

1. Introduction

The carbonic anhydrases (CAs) are metalloenzymes playing an important role in many physiological processes of prokaryotes and eukaryotes. They catalyse the reversible hydration of carbon dioxide to bicarbonate and protons so they are also known as carbonate dehydratases. The family of human carbonic anhydrases (hCAs, EC 4.2.1.1) comprises 16 different α-carbonic anhydrase isoforms, of which there are several cytosolic isoforms (CA I-III, CA VII and CA XIII), five are membrane-bound isoforms (CA IV, CA IX, CA XII, CA XIV and CA XV), two are mitochondrial (CA VA and CA VB) isoforms, and one is secreted into saliva (CA VI). The hCAs are involved in various physiological processes, such as gluconeogenesis, lipogenesis, and ureagenesis. However, abnormal levels or activities of these enzymes have been often associated with different diseases such as cancer, epilepsy, obesity, glaucoma, etc.[1-6]

On this basis several specific CA isoforms have become an interesting target for the design of inhibitors or activators with biomedical applications.[5, 7, 8] Various well-known clinically marketed first generation CA inhibitors (CAIs), such as acetazolamide (**AAZ, 1)** and topiramate (**TMP, 2**) (Chart 1), bind druggable CA isoforms (hCA VII, hCA IX and hCA XIV) as well as ubiquitous hCA I and hCA II isoforms which represent the most common off-targets for the development of selective CAIs lacking in unwanted side-effects. Therefore, the current research on CAIs is focused on the design of new molecules displaying high selectivity towards hCA VII, hCA IX, and hCA XIV over cytosolic hCAII and hCA I isoforms.[9] hCA VII presents a limited distribution, being mainly expressed in the cortex, hippocampus and thalamus regions within the mammalian brain where it is considered involved in generating neuronal excitation and seizures[4, 10] as well as in neuropathic pain control.[11]. hCA IX is expressed in a limited number of normal tissues whereas it is overexpressed in many solid tumors and considered involved in critical processes connected with cancer progression. The expression of hCA IX is strongly up-

regulated by hypoxia via the hypoxia inducible factor–1 (HIF-1) transcription factor. The overexpression of hCA IX induces the pH imbalance of tumor issue contributing significantly to the extracellular acidification of solid tumor; thereby hCA IX inhibitors could specifically bind hypoxic tumor cells expressing this isoform; consequently they have been proposed as antitumor agents.[12-21] Finally, hCA XIV is a transmembrane isozyme with extracellularly oriented active site; it is highly abundant in neurons and axons in the murine and human brain, where it seems to play an important role in modulating excitatory synaptic transmission.[22]

The catalytic domain of all human CA contains a common motif including a Zinc (II) ion that is essential for catalysis and is located at the bottom of a deep cleft.[23] The active Zinc ion is coordinated by three histidine residues (His94, His96 and His119) and water/ hydroxide ion reacting with carbon dioxide to give bicarbonate. The **AAZ** (**1**), **TMP** (**2**) and classical CA inhibitors (CAIs) contain a sulfamide, sulfonamide or sulfamate moiety able to coordinate the metal within the catalytic binding site thus blocking the CA enzymatic activity.[24-37] X-ray crystallographic data confirmed that hCA isoform selectivity is generally controlled by the remaining molecular frame.[36, 38-44] So the high selectivity towards several isoforms is conditioned by profitable interactions between the hydrophobic/hydrophilic residues on the CA cleft and suitable functional groups of the most selective hCAIs.[45-47]

Chart 1 here

Pursuing our interest in the field of hCAIs we previously discovered the *N*-(3,4-dimethoxyphenethyl)-4-sulfamoylbenzamide (**3a**) (Chart 1) as an arylsulfonamide derivative able to bind the CA catalytic site.[48, 49] The proposed mechanism of CA inhibition has been demonstrated by co-crystallization of inhibitor **3a** and hCA II (PDB code 3V7X).[48] As shown in Figure 1, compound **3a** assumed two slightly different conformations. As expected the major interactions of compound **3a** were mediated through

the deeply buried sulfonamide group making polar interactions with Zinc ion and residues located at the bottom of the active site cavity (His 94, His 96, and His 119). Moreover, the benzamide fragment was involved in additional water-mediated interactions with residues Gln92, Pro201, and Thr200. Finally, a methoxy group established a further water-mediated hydrogen bond with residues Gly132 and Gln136. Additional non-polar interactions are formed with Val135, Phe131 and Pro202.

Figure 1 here

Compound **3a** showed relevant inhibitory activity in the nanomolar range (K_i values ranging from 2.7 to 8.7 nM), it showed to be poorly selective toward the druggable isoforms hCA VII, hCA IX, and hCA XIV over ubiquitous hCA I and hCA II.[48]

To overcome the low hCA selectivity of inhibitor **3a** we chose to synthesize new direct analogues which could be characterized by a reduced conformational mobility. Therefore, we herein report the synthesis of isoquinoline derivatives **4** as corresponding cyclic analogues of prototype benzamide **3a** (see Chart 2). Moreover, by shifting the nitrogen atom of isoquinoline ring we planned the synthesis of quinoline derivatives **5** as positional isomers.

Chart 2 here

Thus a set of mono- or dimethoxy-benzene derivatives and corresponding dealkyl-analogs has been prepared and tested to further study the role of substituents on the selectivity against some CA isoforms. These modifications could influence the interaction with hydrophilic/hydrophobic areas of catalytic pocket and control the activity/selectivity against some CA isoforms. X-ray crystallography and molecular modeling have been employed to investigate how the binding pose within the catalytic site contribute to the K_i values as well as CA isoform selectivity.

2. Results and discussion

2.1 *Chemistry*

The title compounds 4-(3,4-dihydroisoquinolin-2(1*H*)-ylcarbonyl)benzenesulfonamides (**4a-e**) and 4-(3,4-dihydroquinolin-1(2*H*)-ylcarbonyl)benzenesulfonamides (**5c-e**) have been synthesized. As depicted in Scheme 1 the coupling between the 4-(aminosulfonyl)benzoic acid **7** and suitable and commercially available 1,2,3,4-tetrahydroisoquinolines **6a,c,e** or 1,2,3,4-tetrahydroquinolines **8c,e** led to the corresponding 4-(3,4-dihydroisoquinolin-2(1*H*)-ylcarbonyl)benzenesulfonamides **4a,c,e**, and 4-(3,4-dihydroquinolin-1(2*H*)-ylcarbonyl)benzenesulfonamides **5c,e**. Then by dealkylation of methoxy derivatives **4a,c** and **5c** we obtained the hydroxyl analogues **4b,d** and **5d**. Following the same procedure the previously reported benzamide **3a** (R^1R^2 = OMe **)**[48] furnished hydroxyl analogue **3b** ((R^1R^2 = OH) in good yields.

Scheme 1 here

The chemical characterization of compounds **3b**, **4a-e**, and **5c-e** was supported by elemental analyses and spectroscopic measurements. Examination of the ^{1}H NMR spectra indicated that isoquinoline derivatives **4a-e** exist as pairs of amide rotamers at room temperature arising from hindered rotation around the amide C–N bond. This phenomenon has been already observed by other researchers in *N*-acyl- and *N*-formyl-tetrahydroisoquinolines.[50]

2.2 CA Inhibition

The CA inhibitory effects of the new arylsulfonamides **3b**, **4a-e**, **5c-e** were measured for human CA I, CA II, CAVII, CA IX and CA XIV; the results are summarized in Table 1 and compared with K_i values of prototype **3a** and two well-known CA inhibitors **AAZ** (**1**) and **TPM** (**2**) as reference compounds. The first analogue *N*-[2-(3,4-dihydroxyphenyl)ethyl]-4-sulfamoylbenzamide (**3b**) displayed lower inhibitory effects than those of parent

compound **3a** towards all screened isoforms with exception of hCA VII. In particular, the compound **3b** was an excellent hCA VII inhibitor with K_i value of 2.4 nM which was similar to that of reference compound **1** (K_i value of 2.5 nM). The isoquinoline derivatives **4a-e** were generally hCA I, hCA II and hCA VII inhibitors (K_i values ranging from 2.8 to 186 nM). The one notable exception to this expected behaviour was that weak inhibition at hCA VII isoform for compounds **4a** and **4b** which exhibited K_is >800 nM. Considering that the corresponding unsubstituted and monosubstituted derivatives **4c-e** displayed excellent inhibition at all studied isoforms with no exception for hCA VII, we could postulate that the presence of two substituents on benzene-fused ring of 1,2,3,4-tetrahydroisoquinoline nucleus determines an impairment of recognition within catalytic site of hCA VII for compound **4a** and **4b**. We also found that the 4-[(6-methoxy-3,4-dihydroquinolin-1(2*H*)-yl)carbonyl]benzenesulfonamide (**5c**) proved to be an unexpected inactive inhibitor (K_i value > 50000 nM at hCA VII) when compared with isoquinoline analogue 4-[(6-methoxy-3,4-dihydroisoquinolin-2(1*H*)-yl)carbonyl]benzenesulfonamide (**4c,** K_i = 3.1 nM). On the contrary the quinoline derivatives **5d** (R_1 = OH, R_2 = H) and **5e** (R_1 = R_2 = H) proved to be potent hCA VII inhibitors and showed similar efficacy of isoquinoline derivatives **4d** and **4e**. Although the new arylsulfonamides **4a-b**, **4e** and **5c** were low nanomolar inhibitors (K_is <10 nM) of tumor-associated isoform hCA IX and brain-distributed hCA XIV to respect reference compounds **1** and **2**, they showed no-selectivity over cytosolic hCA I and/or hCA II isoforms.

Table 1 here

2.3 Structural analysis

To study the molecular features determining the inhibition profiles of this series of new heterocyclic compounds against hCAs, we have determined the crystal structures of the cytosolic dominant isoform hCA II in complex with five carbonylbenzenesulfonamides (**4a**, **4b**, **4e**, **5c**, and **5e)** that display very low K_i values ranging from 4.67 to 7.7 nM. The data

collection and refinement statistics for these five crystal structures, which were deposited into the PDB under codes 4Z1N, 4Z1K, 4Z1J, 4Z1E, and, 4Z0Q are summarized in Table 2. The cocrystal structures showed that the studied carbonylbenzenesulfonamides **4a**, **4b**, **4e**, **5c**, and **5e** were able to occupy all accessible surface of active site funnel. As expected the sulfonamide anchoring group is deeply buried and coordinated to the active site Zinc ion, thus forming the canonical interactions with the enzyme active site reported for other inhibitors as exemplified for inhibitor **3a** in Figure 1. Whereas, the heterocyclic nucleus makes multiple interactions with hydrophilic and hydrophobic surfaces of catalytic site.

Table 2 here

The structures of hCA II in complex with 4-(3,4-dihydroisoquinolin-2(1*H*)-ylcarbonyl)benzenesulfonamides (**4a**, **4b** and **4e**, Figure 2) have been determined at resolution 1.27-1.47 Å and there is no evidence of alternative conformations for any of the inhibitors as observed for the parent compound **3a** (see Figure 1). Despite the different pattern of substitution on benzene fused ring of isoquinoline moiety, we found that the overall binding positions of the three inhibitors **4a**, **4b**, and **4e** within the hCA II catalytic site are nearly superimposable. These structural results are consistent with the observation that the inhibitory K_i values against hCA II are very similar (see Table 1). In Figure 2A we displayed the crystal structures of hCA II in complex with inhibitor **4a** (orange) for which the dynamic disorder of methoxygroups results in poor or missing electron densities for the oxygen atoms of methoxy groups. Figure 2B compares the binding modes of the inhibitors **4b** (yellow) and **4e** (purple) within hCA II cavity. Differently from the inhibitor **4a**, it can be observed that the two inhibitors **4b** and **4e** are unambiguously visible in the electron density maps. In these cocrystal structures the hydrogen bond interaction between carbonyl oxygen and Gln92 are detectable. Remaining contacts between **4b** or **4e** compounds and hCA II are Van der Waals interactions with

each inhibitor and a series of residues: Asn67, Ile91, Gln92, His94, His119, Val121, Phe131, Val 35, Val143, Leu-Thr-Thr-Pro-Pro 198-202, Val 204 and Trp 209. Furthermore, there is an additional hydrogen bond (3.2 Å) formed between phenolic oxygen atom of inhibitor **4b** and water molecules (red spheres) in the first hydration shell of hCA II, no other interaction of the hydroxyl or methoxy analogues has been found.

Figure 2 here

High resolution cocrystal structure of unsubstituted 4-(3,4-dihydroquinolin-1(2*H*)-ylcarbonyl)benzenesulfonamide (**5e**) (1.45 Å) shows that the inhibitor (K_i value of 6.8 nM) assumes three alternative conformations (Figure 3A) fitting in the expanded area located at the top of the active site cavity. When the three binding poses of **5e** are compared to the two poses of its parent compound **3a** cocrystallized with hCA II (PDB code 3V7X[48]) we observe that binding mode of inhibitor **3a** (K_i value of 2.7 nM) overlays the dihydroquinoline ring of **5e**, especially with the most preferred alternative conformation (designated A and indicated by a white arrow in Figure 3B). As expected the inhibitor **5e** establishes a hydrogen bond interaction between the side-chain of Gln192 and carbonyl oxygen linked to the nitrogen atom of quinoline moiety (Figure 3B). Figure 3C reports the crystal structure of the 4-[(6-methoxy-3,4-dihydroquinolin-1(2*H*)-yl)carbonyl]benzenesulfonamide (**5c**) (grey) bound to hCA II determined at resolution 2 Å. The crystallographic analysis furnishes suggestions how the introduction of a methoxy group on benzene fused ring could affect the inhibitor binding mode. Interestingly, inhibitor **5c** (K_i value of 5.69 nM) acquires a single binding mode within the active site of hCA II and adopts an orientation for which the binding of sulfonamide anchor is again the “canonical one”[48]. Although compound **5c** seems to lose the interaction with residue Gln92, the carbonyl oxygen of inhibitor makes hydrogen bond to water molecule from the first hydration shell for which this water molecule is bound to other water molecules interacting to protein atoms. Considering that **5c** and **5e** show very similar K_i values (5.69 nM and 6.8

nM, respectively) we can conclude that this different binding mode does not affect the affinity toward hCA II. In the quest to in depth study the crystal complexes of the two equiactive inhibitors **5c** and **5e** we compared their binding modes (Figure 3C). It emerged that the two sulfonamide moieties show essentially overlapping orientation, whereas the two inhibitors exhibited a different rotated position of quinoline ring in the top area of the catalytic site. The reason for different quinoline moiety placement could be the spatial hindrance of methoxy group of **5c** within the active site of hCA II. We can hypothesize that there are possible clashes with Pro 202 and/or flexible N-terminus. Figure 3C also compares the connections with the protein observed for the three alternative binding poses of inhibitor **5e** (depicted in black line) with the single pose of methoxyanalogue **5c** (in grey stick presentation). It is apparent that the interacting residues might be subdivided into three different groups which are displayed using different colour. The first group assembles the residues interacting with **5c** only (Asn67 and Gln92, coloured in blue); the second group concerns the residues interacting with **5e** only (Trp5, His64, His119 and Leu141, coloured in red); the third group collects all residues that interact with both inhibitors (Gln92, His94, Val121, Phe131, Val135, Val143, Leu-Thr-Thr-Pro-Pro 198-202, Val 204 and Trp209, coloured in magenta). Therefore, despite the different orientations of inhibitors **5c** and **5e** bound to hCA II, they are able to establish profitable interactions with specific and crucial residues of the hydrophobic cleft (Phe131, Val135, Pro202, and Leu204).

In agreement with these data, we can postulate that the expanded surface of hydrophobic area of hCA II allows slight structural modifications in the heterocyclic moiety of studied carbonylbenzenesulfonamides. Actually, in this study all synthesized compounds (**3a-b**, **4a-e**, **5c-e**) show a much flat structure activity relationship not correlated with the nature of substituent (R = H, OMe, OH) on the benzene fused ring. As

observed for methoxyderivative **5c**, the steric constrain could influence the orientation within catalytic pocket without a reduction of affinity.

Figure 3 here

A similar trend was observed for K_i values exhibited towards isoforms hCA IX and hCA XIV for which the hydrophobic cleft is larger than hCA II and probably does not induce good selectivity for this series of inhibitors.[46] On the contrary the same structural modifications seem to have a great influence on hCA VII inhibitory effects. As you can see in Table 1, compounds **4b, 4e** and **5c** are promiscuous, low nanomolar inhibitors, toward hCA II, hCA IX and hCA XIV isoforms; we also found that **4e** was active inhibitor toward hCA VII. Whereas compounds **4b** and **5c** showed unexpectedly loss of inhibitory efficacy toward hCA VII. To better understand these experimental data, computational studies have been performed for the three sulfonamides **4b**, **4e**, and **5c** which were docked into hCA VII catalytic site retrieved from literature (PDB code 3ML5).[51]

Figure 4 here

The superposition of the docking poses of the three inhibitors **4b**, **4e,** and **5c** into the hCA VII (Figure 4, panel) furnished some suggestions about the inhibitory effects toward this specific isoform. It may be observed that the three inhibitors are anchored to the active site through the coordination of Zinc ion by means of one nitrogen atom of the three superimposable sulfonamide groups, whereas the quinoline/isoquinoline nucleus for each molecule adopts a very different orientation. The panel B of Figure 4 displays the crucial interactions with Zinc ion within catalytic site for the active hCA VII inhibitor **4e**, for which we measured binding energy (162.073 kcal mol^{-1}) using Discovery Studio Version 2.5.

We found that the heterocyclic ring of the compound **4e** (blue) lies the hydrophobic cleft (coloured area in magenta) defined by residues Phe131, Ala135, Leu198, Pro202. It is interesting to note that compound **4e** assumes a disposition that is similar to that has been observed in its complex with hCA II isoform. This behaviour could explain the very similar

K_i values measured for the two compared isoforms (7.7 and 9.2 nM, respectively). Moreover, we can speculate that the reduction of hCA VII inhibitory effects observed for compounds **4b** and **5c** could be due to their alternative orientations into hCA VII catalytic site when compared with their binding poses observed into their complexes with hCA II. As shown in Figure 4 the heterocyclic ring of the low active inhibitor **4b** (yellow) seems to occupy the middle area of catalytic channel making weaker interactions with the hydrophobic cleft thus furnishing a plausible explanation of a K_i value of 819 nM. In the case of compound **5c**, coloured in pink, the lack of inhibitory effects might be related to its inability to establish favourable interactions with the before mentioned hydrophobic cleft. Thereby, it is also reasonable that the inhibitory effects are especially related to the distance between heterocyclic ring of each inhibitor and the crucial residue Phe131[52] (highlighted in hydrophobic surface coloured in magenta). On the basis of these findings we hypothesize that for these compounds the residue Phe131 could exert a fine-tuned control of their recognition process into catalytic site of hCA VII.

3. Conclusions

By means of this study we confirmed that the presence of an arylsulfonamide moiety generally led to highly effective CA inhibitors. In fact we have identified a small series of compounds displaying K_i values in the nanomolar range towards druggable hCA isoforms. To decipher the mechanism of inhibitory properties we obtained high resolution crystal structures for selected compounds in complex with hCA II. This X-ray study highlighted the main interactions between the arylsulfonamide moiety and the enzymatic catalytic pocket. Notably, in this series of compounds the two isoquinolines **4a** and **4b** as well as quinoline **5c** showed very weak inhibitory activity against hCA VII. Thus, to explain the reason of this unexpected behaviour we performed molecular docking experiments. It is apparent that remarkable change in inhibitory effects against hCA VII is related to the structural

modification inducing the alteration of the crucial T-shaped π-stacking with the aromatic ring of Phe131 in the hydrophobic cleft. On the contrary the same structural modifications produce weaker influence against other druggable isoforms. In this contribution another relevant finding was the identification of arylsulfonamide compounds lacking of hCA affinity exclusively against hCA VII. Therefore these uncommon CA inhibitors should be useful probe to explore the selectivity profile towards this brain-associated cytosolic CA isoform. Moreover, the potent inhibitory effects of compounds **4a, 4b** and **5c** (K_i values from 5.01 to 6.46 nM) toward tumor-associated hCA IX isoform might be favourably devoid of unwanted-effects in Central Nervous System mediated by hCA VII inhibition. Finally, to improve the selectivity profile our efforts will be devoted to gain low efficacy also toward hCA II that is considered responsible for unwanted-effects of the currently used hCAIs.

4. Experimental section

4.1. Chemistry

All starting materials and reagents were purchased from Sigma-Aldrich Milan, (Italy) and used without further purification. Melting points were determined on a Buchi B-545 apparatus and are uncorrected. By combustion analysis (C, H, N) carried out on a Carlo Erba Model 1106 Elemental Analyzer we determined the purity of synthesized compounds; the results were within ± 0.4 % of the theoretical values. Merck silica gel 60 F254 plates were used for analytical TLC. R_f values were determined on TLC plates using a mixture of DCM/MeOH (94:6) as eluent. Flash Chromatography (FC) was performed on a Biotage SP_1 EXP. ^{1}H NMR and ^{13}C spectra were measured in DMSO-d_6 with a Varian Gemini 300 spectrometer; chemical shifts are expressed in δ (ppm) and coupling constants (J) in Hz. All exchangeable protons were confirmed by addition of deuterium oxide (D_2O). GC-MS spectra for compounds **4c** and **5d** were recorded on a Shimadzu QP500 EI 151 mass spectrometer.

4.1.1. Synthesis of N-[2-(3,4-dihydroxyphenyl)ethyl]-4-sulfamoylbenzamide (3b), 4-(3,4-dihydroisoquinolin-2(1H)-ylcarbonyl)benzenesulfonamides (4a-e), 4-(3,4-dihydroquinolin-1(2H)-ylcarbonyl)benzenesulfonamides (5c-e)

A mixture of 4-(aminosulfonyl)benzoic acid (**7**)(2mmol, 402mg), N,N,N′,N′-tetramethyl-O-(1*H*-benzotriazol-1-yl)uranium hexafluorophosphate (HBTU) (2mmol, 758mg) in dimethylformamide (2 mL) was stirred at room temperature for 1h. Then, a solution of the appropriate 1,2,3,4-tetrahydroisoquinoline (**6a,c,e**) or 1,2,3,4-tetrahydroquinoline (**8c,e**) (2mmol) in TEA (2mmol, 278µl) was added dropwise. The reaction mixture was left overnight and then quenched with water (10 mL) and extracted with EtOAc (3x5 mL). The organic phase was dried with Na_2SO_4 and the solvent was removed in vacuo. The residue was purified by flash chromatography (DCM/MeOH 96:4), crystallized by treatment with diethyl ether and ethanol giving the desired final compounds **4a,c,e** and **5c-e** as white crystals. As starting reagent the benzamide **3a** was re-synthesized following a previously reported procedure and the spectral data was in accordance with literature.[37] The methoxy derivatives **3a**, **4a,c** and **5c**(1 mmol) were dissolved in methylene chloride (DCM) (5 mL), treated with BBr_3 (1 M in DCM) (6 mmol, 6mL) under nitrogen atmosphere and stirred overnight. After completion of the reaction, MeOH (7 mL) was carefully added at 0°C and the solvents removed under reduced pressure. The residue was dissolved in EtOAc (10 mL) and washed with H_2O (10 mL x 3). The organic layer was dried (Na_2SO_4) and concentrated in vacuo. The crude products were crystallized from diethyl ether to give the desired corresponding hydroxy-derivatives **3b**, **4b,d** and **5d**.

4.1.1.1. N-[2-(3,4-Dihydroxyphenyl)ethyl]-4-sulfamoylbenzamide (3b) Yield 63%; mp 204-205℃; R_f= 0.10; ^{1}H NMR (DMSO-d_6): δ 2.63 (t, *J*= *7.8*, 2H, CH_2), 3.38 (t, 2H, CH_2), 6.43-

6.62 (m, 3H, ArH), 7.44 (bs, 2H, NH_2), 7.85 (d, *J= 8.5*, 2H, ArH), 7.93 (d, J= 8.5, 2H, ArH), 8.62 (s, 1H, OH); 8.65 (bs, 1H, NH); 8.73 (s, 1H, OH); Anal. $C_{15}H_{16}N_2O_5S$

4.1.1.2. 4-[(6,7-Dimethoxy-3,4-dihydroisoquinolin-2(1H)-yl)carbonyl]benzenesulfonamide (4a)

Yield 16%; mp 210-212 ℃; R_f = 0.50; ^{1}H NMR (DMSO-d_6): the compound exists as a pair of rotamers at room temperature. δ 2.75 (mc, 2H, major rotamer, CH_2), 2.80 (mc, 2H, minor rotamer, CH_2), 3.48 (mc, 2H, major rotamer, CH_2), 3.72 (s, 3H, OCH_3), 3.74 (s, 3H, OCH_3), 3.84 (mc, 2H, minor rotamer, CH_2), 4.45 (mc, 2H, minor rotamer, CH_2), 4.71 (mc, 2H, major rotamer, CH_2), 6.65 (s, 1H, minor rotamer, ArH), 6.75 (s, 1H, major rotamer, ArH), 6.75 (s, 1H, minor rotamer, ArH), 6.88 (s, 1H, major rotamer, ArH), 7.50 (bs, 2H, NH_2), 7.65 (d, *J= 6.1*, 2H, ArH), 7.90 (d, *J= 8.3*, 2H, ArH); ^{13}C NMR (DMSO) (ppm): δ 27.3, 28.4, 40.3, 43.9, 44.9, 48.8, 55.7, 55.7, 100.1, 109.7, 110.2, 112.1, 124.6, 126.0, 127.5, 127.7, 128.2, 139.6, 144.9, 147.6, 168.1, 168.5. Anal. $C_{18}H_{20}N_2O_5S$.

4.1.1.3. 4-[(6-Methoxy-3,4-dihydroisoquinolin-2(1H)-yl)carbonyl]benzenesulfonamide (4c)

Yield 74%; mp 181-182℃; R_f = 0.46; ^{1}H NMR (DMSO-d_6): the compound exists as a pair of rotamers at room temperature. δ 2.79 (mc, 2H, major rotamer, CH_2), 2.85 (mc, 2H, minor rotamer, CH_2), 3.46 (mc, 2H, major rotamer, CH_2), 3.70 (s, 3H, OCH_3), 3.81 (mc, 2H, minor rotamer, CH_2), 4.42 (mc, 2H, minor rotamer, CH_2), 4.69 (mc, 2H, major rotamer, CH_2), 6.74-7.18 (m, 3H, ArH), 7.47 (bs, 2H, NH_2), 7.63 (d, *J= 7.7*, 2H, ArH), 7.87 (d, *J*= 8.2, 2H, ArH); GC-MS (EI) m/z (%): 346 (M^+, 0), 222 (4.3), 194 (0.5), 177 (35), 176 (18), 164 (0.5), 150 (15), 149 (100), 121 (6.2), 105 (7.8); Anal. $C_{17}H_{18}N_2O_4S$.

4.1.1.4. 4-(3,4-Dihydroisoquinolin-2(1H)-ylcarbonyl)benzenesulfonamide (4e)

Yield 20%; mp 215-217℃; R_f = 0.51; ^{1}H NMR (DMSO-*d_6*): the compound exists as a pair of rotamers at room temperature. δ 2.90 (mc, 2H, major rotamer, CH_2), 2.95 (mc, 2H, minor rotamer, CH_2), 3.57 (mc, 2H, major rotamer, CH_2), 3.92 (mc, 2H, minor rotamer, CH_2), 4.57 (mc, 2H, minor rotamer, CH_2), 4.84 (mc, 2H, major rotamer, CH_2), 7.07-7.32 (mc, 4H, ArH), 7.53 (bs, 2H, NH_2), 7.70 (d, *J= 6.4*, 2H, ArH), 7.95 (d, *J= 8.3*, 2H, ArH); ^{13}C NMR (DMSO) (ppm): δ 27.6, 28.7, 40.1, 44.1, 44.6, 48.8, 125.9, 127.3, 128.6, 132.8, 134.1, 135,4, 139.3, 144.8, 168.0, 168.4. Anal. $C_{16}H_{16}N_2O_3S$.

4.1.1.5. 4-[(6-Methoxy-3,4-dihydroquinolin-1(2H)-yl)carbonyl]benzenesulfonamide (5c)

Yield 69%; mp 176-177℃; R_f = 0.52; ^{1}H NMR (DMSO-*d_6*): δ 1.94 (t, 2H, CH_2), 2.80 (t, 2H, CH_2), 3.69 (s, 3H, OCH_3), 3.72 (s, 2H, CH_2), 6.81 (mc, 1H, ArH), 7.46 (bs, 2H, NH_2), 7.50 (d, *J*= 7.7, 2H, ArH), 7.76 (d, *J*= 8.2, 2H, ArH); Anal. $C_{17}H_{18}N_2O_4S$.

4.1.1.6. 4-(3,4-Dihydroquinolin-1(2H)-ylcarbonyl)benzenesulfonamide (5e)

Yield 16%; mp 225-227℃; R_f = 0.61; ^{1}H NMR (DMSO-*d_6*): δ 1.94 (q, 2H, CH_2), 2.81 (t, 2H, CH_2), 3.73 (t, 2H, CH_2), 6.87-7.21 (m, 4H, ArH), 7.44 (bs, 2H, NH_2), 7.50 (d, *J= 8.3*, 2H, ArH), 7.74 (d, *J= 8.3*, 2H, ArH); Anal. $C_{16}H_{16}N_2O_3S$.

4.1.1.7. 4-[(6,7-Dihydroxy-3,4-dihydroisoquinolin-2(1H)-yl)carbonyl]benzenesulfonamide (4b)

Yield 60%; mp 240-243 ℃; R_f = 0.52. ^{1}H NMR (DMSO-*d_6*): the compound exists as a pair of rotamers at room temperature. δ 2.64 (mc, 2H, major rotamer, CH_2), 2.69 (mc, 2H, , minor rotamer, CH_2), 3.43 (mc, 2H, major rotamer, CH_2), 3.79 (mc, 2H, minor rotamer, CH_2), 4.31 (mc, 2H, minor rotamer, CH_2), 4.59 (mc, 2H, major rotamer, CH_2), 6.52 (mc,

1H, ArH), 6.59 (mc, 1H, ArH), 7.49 (bs, 2H, NH_2), 7.63 (d, *J*= *7.7*, 2H, ArH), 7.89 (d, *J*= *8.3*, 2H, ArH), 8.83 (s, 2H, OH); Anal. $C_{16}H_{16}N_2O_5S$.

4.1.1.8. 4-[(6-Hydroxy-3,4-dihydroisoquinolin-2(1H)-yl)carbonyl]benzenesulfonamide (4d)

Yield 92%; mp 222-223℃; R_f = 0.24; ^{1}H NMR (DMSO-d_6): the compound exists as a pair of rotamers at room temperature. δ 2.74 (mc, 2H, major rotamer, CH_2), 2.80 (mc, 2H, minor rotamer, CH_2), 3.47 (mc, 2H, major rotamer, CH_2), 3.82 (mc, 2H, minor rotamer, CH_2), 4.40 (mc, 2H, minor rotamer, CH_2), 4.67 (mc, 2H, major rotamer, CH_2), 6.57–7.08 (m, 3H, ArH), 7.49 (bs, 2H, NH_2), 7.65 (d, *J*= 8.2, 2H, ArH), 7.90 (d, *J*= 8.2, 2H, ArH), 9.29 (s, 1H, OH); Anal. $C_{16}H_{16}N_2O_4S$.

4.1.1.9. 4-[(6-Hydroxy-3,4-dihydroquinolin-1(2H)-yl)carbonyl]benzenesulfonamide (5d)

Yield 44%; mp 229-230℃; R_f = 0.26; ^{1}H NMR (DMSO-d_6): δ 1.92 (t, 2H, CH_2), 2.73 (t, 2H, CH_2), 3.69 (d, 2H, CH_2), 6.59 (m, 3H, ArH), 7.45 (bs, 2H, NH_2), 7.46 (mc, 2H, ArH), 7.75 (d, 2H, ArH),9.30 (s, 1H, OH); 332 (M^+, 0), 222 (3.5), 194 (0.5), 177 (32), 176 (16), 164 (0.5), 150 (14), 149 (100), 121 (5.8), 105 (7.7); Anal. $C_{16}H_{16}N_2O_4S$.

4.2. CA Inhibition Assay

An Applied Photophysics stopped-flow instrument has been used for assaying the CA catalysed CO_2 hydration activity. Phenol red (at a concentration of 0.2 mM) has been used as indicator, working at the absorbance maximum of 557 nm, with 10 – 20 mMHepes (pH 7.5) or Tris (pH 8.3) as buffers, and 20 mM Na_2SO_4 or 20 mM $NaClO_4$ (for maintaining constant the ionic strength), following the initial rates of the CA-catalyzed CO_2 hydration reaction for a period of 10-100 s. The CO_2 concentrations ranged from 1.7 to 17 mM for the determination of the kinetic parameters and inhibition constants. For each inhibitor at least six traces of the initial 5-10% of the reaction have been used for determining the

initial velocity. The uncatalyzed rates were determined in the same manner and subtracted from the total observed rates. Stock solutions of inhibitor (10 mM) were prepared in distilled-deionized water and dilutions up to 0.01 nM were done thereafter with distilled-deionized water. Inhibitor and enzyme solutions were preincubated together for 15 min at room temperature prior to assay, in order to allow for the formation of the E-I complex. The inhibition constants were obtained by non-linear least-squares methods using PRISM 3, as reported earlier, and represent the mean from at least three different determinations. CA isoforms were recombinant ones obtained as reported earlier by this group.[53-56]

4.3. Protein Crystallography

4.3.1. Protein Crystallization and Diffraction Data Collection. Co-crystals of human carbonic anhydrase II (purchased from Sigma, catalog No. C6165) with compounds **4a, 4b, 4e, 5c** and **5e** are obtained by vapor-diffusion hanging drop method at 18 °C. Complexes were prepared by adding 2 or 3.5-fold molar excess of inhibitor (dissolved in pure DMSO) to 12-13 mgxmL^{-1} protein solution in water. 2 µL of complex solution were mixed with 2 µL of precipitant solution containing 1,6M sodium citrate, 50mM Tris HCl pH 7.8 and equilibrated over a 1 mL reservoir of precipitant solution. The final DMSO concentration did not exceed 1.5 % (v/v). Crystals with dimensions of 0.5 mm × 0.3 mm × 0.2 mm grew within 2 weeks. Before data collection, the crystals were soaked for 5-10 s in reservoir solution supplemented with 25 % (v/v) glycerol and stored in liquid N_2. Diffraction data for crystallized complexes CAII-**4a,b,e** and **5e** were collected at 100 K at beamline MX14.2 of BESSY, Berlin, Germany [57] and these diffraction data were integrated and reduced using XDS program [58] and its graphical interface XDSAPP [59]. Diffraction data of crystallized complex CAII-**5c** were collected to 2.0 Å resolution at 120 K using an in-house diffractometer (Nonius FR 591) connected to 345 mm MarResearch image plate detector. Diffraction data were integrated and reduced using MOSFLM[60] and scaled

using SCALA[61] from the CCP4 suite of programs.[62] Crystal parameters and data collection statistics for both complexes are summarized in Table 2.

4.3.2. Structure Determination, Refinement, and Analysis. The structures of hCA II complexes were solved using the difference Fourier technique, using hCA II structure (Protein Data Bank entry 3PO6 [36]) as the initial model. Initial rigid-body refinement and subsequent restrained refinement for both hCA II complexes were performed using the program REFMAC5[62] with isotropic ADPs. The structures were refined with one inhibitor molecule in the enzyme active site with occupancy 1, however for the compound **5e**, the model of inhibitor molecule was build up in three partially different alternative conformations. Atomic coordinates and geometric library for the inhibitor were generated using the PRODRG server[63]. The Coot program[64] was used for inhibitor fitting, model rebuilding, and addition of water molecules. All structures were first refined with isotropic ADPs. After addition of solvent atoms, metal ions (zinc), building inhibitor molecules in the active site, and several alternate conformations for a number of residues, anisotropic ADPs were refined for nearly all atoms for the complexes CAII-4b,e and 5e (with the exception of spatially overlapping atoms in segments with alternate conformations; also oxygen atoms of water molecules with unrealistic ratio of ellipsoid axes were refined with isotropic ADPs) including the inhibitor molecules. For the complexes CAII-**4a** and **5c** the refinement was finished using isotropic ADPs. The quality of the crystallographic model was assessed with MolProbity.[65] The final refinement statistics are summarized in Table 2. All figures showing structural representations were prepared using PYMOL Molecular Graphics System (Version 1.3r1 Schrodinger, LLC. 2010).

4.4. Molecular docking

The crystal structures of hCA VII in complex with the inhibitor acetazolamide was retrieved from the RCSB Protein Data Bank (PDB: 3ML5) [51]. The ligand and water molecules were discarded, and the hydrogen atoms were added to protein with Discovery Studio 2.5.5.[66] The structures of the ligands were constructed using Discovery Studio 2.5.5 and energy minimized using the Smart Minimizer protocol (1000 steps) which combines the Steepest Descent and the Conjugate Gradient methods. The ligands minimized in this way were docked in their corresponding proteins by means of Gold Suite 5.0.1.[67] The region of interest used by Gold program was defined in order to contain the residues within 10 Å from the original position of the ligand in the X-ray structure. A scaffold constraint (penalty = 10.0) was used to restrict the solutions in which the sulfonamide moiety was able to coordinate the metal within the catalytic binding site. GoldScore was chosen as fitness function and the standard default setting were used in all calculations and the ligands were submitted to 100 genetic algorithm runs. The “allow early termination” command was deactivated. Results differing by less than 0.75 Å in ligand-all atom RMSD, were clustered together. The best GOLD-calculated conformation was used both for analysis and representation.

Acknowledgments

Financial support for this research by Fondo di Ateneo per la Ricerca (PRA grant number ORME09SPNC - Università di Messina)

References

[1] C.T. Supuran, Diuretics: from classical carbonic anhydrase inhibitors to novel applications of the sulfonamides, Curr. Pharm. Des. 14 (2008) 641-648.

[2] F. Mincione, A. Scozzafava, C.T. Supuran, The development of topically acting carbonic anhydrase inhibitors as antiglaucoma agents, Curr. Pharm. Des. 14 (2008) 649-654.

[3] G. De Simone, A. Di Fiore, C.T. Supuran, Are carbonic anhydrase inhibitors suitable for obtaining antiobesity drugs?, Curr. Pharm. Des. 14 (2008) 655-660.

[4] A. Thiry, J.M. Dogne, C.T. Supuran, B. Masereel, Carbonic anhydrase inhibitors as anticonvulsant agents, Curr. Top. Med. Chem. 7 (2007) 855-864.

[5] C.T. Supuran, Inhibition of bacterial carbonic anhydrases and zinc proteases: from orphan targets to innovative new antibiotic drugs, Curr. Med. Chem. 19 (2012) 831-844.

[6] B. Bao, K. Groves, J. Zhang, E. Handy, P. Kennedy, G. Cuneo, C.T. Supuran, W. Yared, M. Rajopadhye, J.D. Peterson, In vivo imaging and quantification of carbonic anhydrase IX expression as an endogenous biomarker of tumor hypoxia, PLoS One 7 (2012) e50860.

[7] C.T. Supuran, Carbonic anhydrase inhibitors as emerging drugs for the treatment of obesity, Expert Opin. Emerg. Drugs 17 (2012) 11-15.

[8] C.T. Supuran, Carbonic anhydrases: novel therapeutic applications for inhibitors and activators, Nat. Rev. Drug Discov. 7 (2008) 168-181.

[9] V. Alterio, A. Di Fiore, K. D'Ambrosio, C.T. Supuran, G. De Simone, Multiple binding modes of inhibitors to carbonic anhydrases: how to design specific drugs targeting 15 different isoforms?, Chem. Rev. 112 (2012) 4421-4468.

[10] A. Thiry, B. Masereel, J.M. Dogne, C.T. Supuran, J. Wouters, C. Michaux, Exploration of the binding mode of indanesulfonamides as selective inhibitors of human carbonic anhydrase type VII by targeting Lys 91, ChemMedChem 2 (2007) 1273-1280.

[11] R. Demirdag, V. Comakli, M. Senturk, D. Ekinci, O. Irfan Kufrevioglu, C.T. Supuran, Purification and characterization of carbonic anhydrase from sheep kidney and effects of sulfonamides on enzyme activity, Bioorg. Med. Chem. 21 (2013) 1522-1525.

[12] I. Nishimori, D. Vullo, T. Minakuchi, A. Scozzafava, C. Capasso, C.T. Supuran, Restoring catalytic activity to the human carbonic anhydrase (CA) related proteins VIII, X and XI affords isoforms with high catalytic efficiency and susceptibility to anion inhibition, Bioorg. Med. Chem. Lett. 23 (2013) 256-260.

[13] H.M. Said, C.T. Supuran, C. Hageman, A. Staab, B. Polat, A. Katzer, A. Scozzafava, J. Anacker, M. Flentje, D. Vordermark, Modulation of carbonic anhydrase 9 (CA9) in human brain cancer, Curr. Pharm. Des. 16 (2010) 3288-3299.

[14] O.O. Guler, G. De Simone, C.T. Supuran, Drug design studies of the novel antitumor targets carbonic anhydrase IX and XII, Curr. Med. Chem. 17 (2010) 1516-1526.

[15] V. Akurathi, L. Dubois, N.G. Lieuwes, S.K. Chitneni, B.J. Cleynhens, D. Vullo, C.T. Supuran, A.M. Verbruggen, P. Lambin, G.M. Bormans, Synthesis and biological evaluation of a 99mTc-labelled sulfonamide conjugate for in vivo visualization of carbonic anhydrase IX expression in tumor hypoxia, Nucl. Med. Biol. 37 (2010) 557-564.

[16] C. Genis, K.H. Sippel, N. Case, W. Cao, B.S. Avvaru, L.J. Tartaglia, L. Govindasamy, C. Tu, M. Agbandje-McKenna, D.N. Silverman, C.J. Rosser, R. McKenna, Design of a carbonic anhydrase IX active-site mimic to screen inhibitors for possible anticancer properties, Biochemistry 48 (2009) 1322-1331.

[17] A. Thiry, C.T. Supuran, B. Masereel, J.M. Dogne, Recent developments of carbonic anhydrase inhibitors as potential anticancer drugs, J. Med. Chem. 51 (2008) 3051-3056.

[18] S. Pastorekova, J. Kopacek, J. Pastorek, Carbonic anhydrase inhibitors and the management of cancer, Curr. Top. Med. Chem. 7 (2007) 865-878.

[19] G. De Simone, R.M. Vitale, A. Di Fiore, C. Pedone, A. Scozzafava, J.L. Montero, J.Y. Winum, C.T. Supuran, Carbonic anhydrase inhibitors: Hypoxia-activatable sulfonamides incorporating disulfide bonds that target the tumor-associated isoform IX, J. Med. Chem. 49 (2006) 5544-5551.

[20] T.W. Meijer, J. Bussink, M. Zatovicova, P.N. Span, J. Lok, C.T. Supuran, J.H. Kaanders, Tumor Microenvironmental Changes Induced by the Sulfamate Carbonic Anhydrase IX Inhibitor S4 in a Laryngeal Tumor Model, PLoS One 9 (2014) e108068.

[21] N. Krall, F. Pretto, W. Decurtins, G.J. Bernardes, C.T. Supuran, D. Neri, A small-molecule drug conjugate for the treatment of carbonic anhydrase IX expressing tumors, Angew. Chem. Int. Ed. Engl. 53 (2014) 4231-4235.

[22] S. Parkkila, A.K. Parkkila, H. Rajaniemi, G.N. Shah, J.H. Grubb, A. Waheed, W.S. Sly, Expression of membrane-associated carbonic anhydrase XIV on neurons and axons in mouse and human brain, Proc. Natl .Acad. Sci. U S A 98 (2001) 1918-1923.

[23] J.Y. Winum, C.T. Supuran, Recent advances in the discovery of zinc-binding motifs for the development of carbonic anhydrase inhibitors, J. Enzyme Inhib. Med. Chem. (2014) 1-4.

[24] F. Carta, A. Scozzafava, C.T. Supuran, Sulfonamides: a patent review (2008 - 2012), Expert Opin. Ther. Pat. 22 (2012) 747-758.

[25] K. D'Ambrosio, F.Z. Smaine, F. Carta, G. De Simone, J.Y. Winum, C.T. Supuran, Development of potent carbonic anhydrase inhibitors incorporating both sulfonamide and sulfamide groups, J. Med. Chem. 55 (2012) 6776-6783.

[26] A.M. Marini, A. Maresca, M. Aggarwal, E. Orlandini, S. Nencetti, F. Da Settimo, S. Salerno, F. Simorini, C. La Motta, S. Taliani, E. Nuti, A. Scozzafava, R. McKenna, A. Rossello, C.T. Supuran, Tricyclic sulfonamides incorporating benzothiopyrano[4,3-c]pyrazole and pyridothiopyrano[4,3-c]pyrazole effectively inhibit alpha- and beta-

carbonic anhydrase: X-ray crystallography and solution investigations on 15 isoforms, J. Med. Chem. 55 (2012) 9619-9629.

[27] C.T. Supuran, Carbonic anhydrase inhibitors, Bioorg. Med. Chem. Lett. 20 (2010) 3467-3474.

[28] C.T. Supuran, Carbonic anhydrases: again, and again, and again, Curr. Pharm. Des. 16 (2010) 3231-3232.

[29] C.T. Supuran, Carbonic anhydrase inhibition/activation: trip of a scientist around the world in the search of novel chemotypes and drug targets, Curr. Pharm. Des. 16 (2010) 3233-3245.

[30] J. Schulze Wischeler, A. Innocenti, D. Vullo, A. Agrawal, S.M. Cohen, A. Heine, C.T. Supuran, G. Klebe, Bidentate Zinc chelators for alpha-carbonic anhydrases that produce a trigonal bipyramidal coordination geometry, ChemMedChem 5 (2010) 1609-1615.

[31] J.Y. Winum, A. Scozzafava, J.L. Montero, C.T. Supuran, Therapeutic potential of sulfamides as enzyme inhibitors, Med. Res. Rev. 26 (2006) 767-792.

[32] J.Y. Winum, A. Scozzafava, J.L. Montero, C.T. Supuran, Sulfamates and their therapeutic potential, Med. Res. Rev. 25 (2005) 186-228.

[33] N. Pala, L. Micheletto, M. Sechi, M. Aggarwal, F. Carta, R. McKenna, C.T. Supuran, Carbonic Anhydrase Inhibition with Benzenesulfonamides and Tetrafluorobenzenesulfonamides Obtained via Click Chemistry, ACS Med. Chem. Lett. 5 (2014) 927-930.

[34] F. Carta, C.T. Supuran, A. Scozzafava, Sulfonamides and their isosters as carbonic anhydrase inhibitors, Future Med. Chem. 6 (2014) 1149-1165.

[35] R. Gitto, S. Agnello, S. Ferro, L. De Luca, D. Vullo, J. Brynda, P. Mader, C.T. Supuran, A. Chimirri, Identification of 3,4-Dihydroisoquinoline-2(1H)-sulfonamides as

potent carbonic anhydrase inhibitors: synthesis, biological evaluation, and enzyme--ligand X-ray studies, J. Med. Chem. 53 (2010) 2401-2408.

[36] P. Mader, J. Brynda, R. Gitto, S. Agnello, P. Pachl, C.T. Supuran, A. Chimirri, P. Rezacova, Structural basis for the interaction between carbonic anhydrase and 1,2,3,4-tetrahydroisoquinolin-2-ylsulfonamides, J. Med. Chem. 54 (2011) 2522-2526.

[37] R. Gitto, S. Agnello, S. Ferro, D. Vullo, C.T. Supuran, A. Chimirri, Identification of potent and selective human carbonic anhydrase VII (hCA VII) inhibitors, ChemMedChem 5 (2010) 823-826.

[38] K.M. Jude, A.L. Banerjee, M.K. Haldar, S. Manokaran, B. Roy, S. Mallik, D.K. Srivastava, D.W. Christianson, Ultrahigh resolution crystal structures of human carbonic anhydrases I and II complexed with "two-prong" inhibitors reveal the molecular basis of high affinity, J. Am. Chem. Soc. 128 (2006) 3011-3018.

[39] S.Z. Fisher, L. Govindasamy, N. Boyle, M. Agbandje-McKenna, D.N. Silverman, G.M. Blackburn, R. McKenna, X-ray crystallographic studies reveal that the incorporation of spacer groups in carbonic anhydrase inhibitors causes alternate binding modes, Acta Crystallogr. Sect. F Struc.t Biol .Cryst. Commun. 62 (2006) 618-622.

[40] V. Alterio, R.M. Vitale, S.M. Monti, C. Pedone, A. Scozzafava, A. Cecchi, G. De Simone, C.T. Supuran, Carbonic anhydrase inhibitors: X-ray and molecular modeling study for the interaction of a fluorescent antitumor sulfonamide with isozyme II and IX, J. Am. Chem. Soc. 128 (2006) 8329-8335.

[41] V. Menchise, G. De Simone, V. Alterio, A. Di Fiore, C. Pedone, A. Scozzafava, C.T. Supuran, Carbonic anhydrase inhibitors: stacking with Phe131 determines active site binding region of inhibitors as exemplified by the X-ray crystal structure of a membrane-impermeant antitumor sulfonamide complexed with isozyme II, J. Med. Chem. 48 (2005) 5721-5727.

[42] M. Bozdag, M. Ferraroni, E. Nuti, D. Vullo, A. Rossello, F. Carta, A. Scozzafava, C.T. Supuran, Combining the tail and the ring approaches for obtaining potent and isoform-selective carbonic anhydrase inhibitors: solution and X-ray crystallographic studies, Bioorg Med Chem 22 (2014) 334-340.

[43] A. Di Fiore, S.M. Monti, M. Hilvo, S. Parkkila, V. Romano, A. Scaloni, C. Pedone, A. Scozzafava, C.T. Supuran, G. De Simone, Crystal structure of human carbonic anhydrase XIII and its complex with the inhibitor acetazolamide, Proteins 74 (2009) 164-175.

[44] V. Alterio, M. Hilvo, A. Di Fiore, C.T. Supuran, P. Pan, S. Parkkila, A. Scaloni, J. Pastorek, S. Pastorekova, C. Pedone, A. Scozzafava, S.M. Monti, G. De Simone, Crystal structure of the catalytic domain of the tumor-associated human carbonic anhydrase IX, Proc. Natl. Acad. Sci. USA 106 (2009) 16233-16238.

[45] J. Moeker, B.P. Mahon, L.F. Bornaghi, D. Vullo, C.T. Supuran, R. McKenna, S.A. Poulsen, Structural Insights into Carbonic Anhydrase IX Isoform Specificity of Carbohydrate-Based Sulfamates, J. Med. Chem. (2014).

[46] G. De Simone, G. Pizika, S.M. Monti, A. Di Fiore, J. Ivanova, I. Vozny, P. Trapencieris, R. Zalubovskis, C.T. Supuran, V. Alterio, Hydrophobic substituents of the phenylmethylsulfamide moiety can be used for the development of new selective carbonic anhydrase inhibitors, Biomed. Res. Int. 2014 (2014) 523210.

[47] V. Alterio, P. Pan, S. Parkkila, M. Buonanno, C.T. Supuran, S.M. Monti, G. De Simone, The structural comparison between membrane-associated human carbonic anhydrases provides insights into drug design of selective inhibitors, Biopolymers 101 (2014) 769-778.

[48] R. Gitto, F.M. Damiano, P. Mader, L. De Luca, S. Ferro, C.T. Supuran, D. Vullo, J. Brynda, P. Rezacova, A. Chimirri, Synthesis, structure-activity relationship studies,

and X-ray crystallographic analysis of arylsulfonamides as potent carbonic anhydrase inhibitors, J. Med. Chem. 55 (2012) 3891-3899.

[49] L. De Luca, S. Ferro, F.M. Damiano, C.T. Supuran, D. Vullo, A. Chimirri, R. Gitto, Structure-based screening for the discovery of new carbonic anhydrase VII inhibitors, Eur. J. Med. Chem. 71 (2014) 105-111.

[50] C.B. de Koning, W.A.L. van Otterlo, J.P. Michael, Amide rotamers of N-acetyl-1,3-dimethyltetrahydroisoquinolines: synthesis, variable temperature NMR spectroscopy and molecular modelling, Tetrahedron 59 (2003) 8337-8345.

[51] A. Di Fiore, E. Truppo, C.T. Supuran, V. Alterio, N. Dathan, F. Bootorabi, S. Parkkila, S.M. Monti, G. De Simone, Crystal structure of the C183S/C217S mutant of human CA VII in complex with acetazolamide, Bioorg. Med. Chem. Lett. 20 (2010) 5023-5026.

[52] M. Bozdag, M. Ferraroni, F. Carta, D. Vullo, L. Lucarini, E. Orlandini, A. Rossello, E. Nuti, A. Scozzafava, E. Masini, C.T. Supuran, Structural insights on carbonic anhydrase inhibitory action, isoform selectivity, and potency of sulfonamides and coumarins incorporating arylsulfonylureido groups, J. Med. Chem. 57 (2014) 9152-9167.

[53] I. Nishimori, D. Vullo, A. Innocenti, A. Scozzafava, A. Mastrolorenzo, C.T. Supuran, Carbonic anhydrase inhibitors: inhibition of the transmembrane isozyme XIV with sulfonamides, Bioorg. Med. Chem. Lett. 15 (2005) 3828-3833.

[54] I. Nishimori, D. Vullo, A. Innocenti, A. Scozzafava, A. Mastrolorenzo, C.T. Supuran, Carbonic anhydrase inhibitors. The mitochondrial isozyme VB as a new target for sulfonamide and sulfamate inhibitors, J. Med. Chem. 48 (2005) 7860-7866.

[55] A. Innocenti, D. Vullo, J. Pastorek, A. Scozzafava, S. Pastorekova, I. Nishimori, C.T. Supuran, Carbonic anhydrase inhibitors. Inhibition of transmembrane isozymes XII (cancer-associated) and XIV with anions, Bioorg. Med. Chem. Lett. 17 (2007) 1532-1537.

[56] I. Nishimori, T. Minakuchi, K. Morimoto, S. Sano, S. Onishi, H. Takeuchi, D. Vullo, A. Scozzafava, C.T. Supuran, Carbonic anhydrase inhibitors: DNA cloning and inhibition studies of the alpha-carbonic anhydrase from Helicobacter pylori, a new target for developing sulfonamide and sulfamate gastric drugs, J. Med. Chem. 49 (2006) 2117-2126.

[57] U. Mueller, N. Darowski, M.R. Fuchs, R. Forster, M. Hellmig, K.S. Paithankar, S. Puhringer, M. Steffien, G. Zocher, M.S. Weiss, Facilities for macromolecular crystallography at the Helmholtz-Zentrum Berlin, J. Synchrotron Rad. 19 (2012) 442-449.

[58] W. Kabsch, Xds, Acta Crystallographica Section D-Biological Crystallography 66 (2010) 125-132.

[59] M. Krug, M.S. Weiss, U. Heinemann, U. Mueller, XDSAPP: a graphical user interface for the convenient processing of diffraction data using XDS, J. Appl. Crystall. 45 (2012) 568-572.

[60] A.G. Leslie, Integration of macromolecular diffraction data, Acta Crystallogr. Sect. D Biol. Crystallogr. 55 (1999) 1696-1702.

[61] P.R. Evans, Proceedings of the CCP4 Study Weekend. Data Collection and Processing, in: L. Sawyer, N. Isaacs, S. Bailey (Eds.), Warrington: Daresbury Laboratory, 1993, pp. 114-122.

[62] The CCP4 suite: programs for protein crystallography, Acta Crystallogr. Sect.D 50 (1994) 760-763.

[63] A.W. Schuttelkopf, D.M. van Aalten, PRODRG: a tool for high-throughput crystallography of protein-ligand complexes, Acta Crystallogr. D Biol. Crystallogr. 60 (2004) 1355-1363.

[64] P. Emsley, K. Cowtan, Coot: model-building tools for molecular graphics, Acta Crystallogr. D Biol. Crystallogr. 60 (2004) 2126-2132.

[65] S.C. Lovell, I.W. Davis, W.B. Arendall, 3rd, P.I. de Bakker, J.M. Word, M.G. Prisant, J.S. Richardson, D.C. Richardson, Structure validation by Calpha geometry: phi,psi and Cbeta deviation, Proteins 50 (2003) 437-450.

[66] Discovery Studio, Accelrys, http://www.accelrys.com, San Diego, CA USA, 2009.

[67] G. Jones, P. Willett, R.C. Glen, A.R. Leach, R. Taylor, Development and validation of a genetic algorithm for flexible docking, J. Mol. Biol. 267 (1997) 727-748.

Table 1. K_i values (nM) against hCA I, hCA II, hCA VII, hCA IX and hCA XIV isoforms showed by arylsulfonamide derivatives **3-5**, acetazolamide (AAZ, **1**), and topiramate (TPM, **2**).

	K_i(nM)[a]				
	hCA I	**hCA II**	**hCA VII**	**hCA IX**	**hCA XIV**
3a[b]	8.7	2.7	5.8	3.8	4.3
3b	31	11.2	2.4	17	58
4a	39.9	5.89	878	6.1	7.2
4b	8.5	4.7	819	5.01	5.8
4c	29	9.5	3.1	27	65
4d	186	10.4	2.8	28	61
4e	76.2	7.7	9.2	7.5	9.6
5c	18.5	5.7	n.d.[c]	6.5	7.9
5d	58	15.1	4.0	42	64
5e	78.6	6.8	8.5	9.4	39.0
1, AAZ[b]	250	12	2.5	25	41
2, TPM[b]	250	10	0.9	58	1460

[a]Errors in the range of ± 10 % of the reported value, from 3 different assays. Recombinant full length hCA I, II VII and XIV and catalytic domain of hCA IX were used. [b] Data are taken from Reference 48. [c] n.d. = not detectable (IC_{50} >50000 nM)

Table 2. Data collection statistics and refinement statistics

	hCA II in complex with				
	4a	**4b**	**4e**	**5c**	**5e**
Crystal parameters and diffraction data statistics					
space group	$P2_1$	$P2_1$	$P2_1$	$P2_1$	$P2_1$
unit cell parameters	FD3	FD4	FD2	FD5	FD1
a, b, c (Å)	42.2 41.3 72.4	42.1 41.3 72.1	42.1 41.2 72.2	42.4 41.45 72.3	42.2 41.7 72.4
α, β, γ (º)	90 104.5 90	90 104.4 90	90 104.3 90	90 104.4 90	90 104.6 90
wavelength (Å)	0.91841	0.97565	0.97565	1.54179	0.97565
resolution range (Å)	50.0-1.47 (1.56-1.47)	50.0-1.35 (1.43-1.35)	50.0-1.27 (1.35-1.27)	41.5-2.0 (2.05-2.00)	50.0-1.45 (1.54-1.45)
No. of unique reflections	69904	92993 (14462)	99304 (12514)	14005 (653)	43348 (6886)
multiplicity	1.3(1.3)	2.1(2.1)	2.2(2.1)	3.8(3.1)	3.7(3.6)
completeness (%)	86.6(81.5)	89.9(86.4)	79.8(62.2)	88.0(90.3)	99.7(99.1)
R_{merge} [a] (%)	10.9 (44.0)	3.8 (44.8)	3.8 (28.7)	6.4 (25.9)	7.9 (56.0)
average I/σ (I)	6.4 (2.2)	14.1 (1.9)	13.7 (3.0)	7.9 (2.8)	11.6 (2.4)
Wilson B ($Å^2$)	16.3	19.1	9.2	23.5	18.4

Refinement statistics	**4a**	**4b**	**4e**	**5c**	**5e**
Resolution range	39.93-1.47 (1.51-1.47)	39.80-1.35 (1.39-1.35)	40.81-1.27 (1.30-1.27)	41.33-2.00 (2.06-2.00)	40.90-1.45 (1.49-1.45)
No. of reflections in working set	35900 (2595)	47453 (3560)	53546 (2857)	13036 (1009)	39013 (2854)
No. of reflections in test set	1995 (137)	2637 (189)	2975 (150)	732 (63)	2168 (150)
R [b] (%)	18.8(26.9)	13.4(20.2)	13.7(17.0)	17.2(20.1)	14.9(18.4)
R_{free} [c] (%)	21.3(31.4)	17.0(26.0)	17.0(22.4)	24.4(23.7)	19.1(24.5)
RMSD bond length (Å)	0.019	0.012	0.013	0.013	0.017
Mean ADP protein/inhibitor ($Å^2$)	11.7	16.1	14.2	13.4	13.8
PDB code	**4Z1N**	**4Z1K**	**4Z1J**	**4Z1E**	**4Z0Q**

[a] $R_{merge} = \Sigma_{hkl}\Sigma_i|I_i(hkl) - \langle I(hkl)\rangle|/\Sigma_{hkl}\Sigma_i I_i(hkl)$, where the $I_i(hkl)$ is an individual intensity of the ith observation of reflection hkl and $\langle I(hkl)\rangle$ is the average intensity of reflection hkl with summation over all data.
[b] $R = ||F_o| - |F_c||/|F_o|$, where F_o and F_c are the observed and calculated structure factors, respectively.
[c] R_{free} is equivalent to R value but is calculated for 5 % of the reflections chosen at random and omitted from the refinement process.

Chart 1.

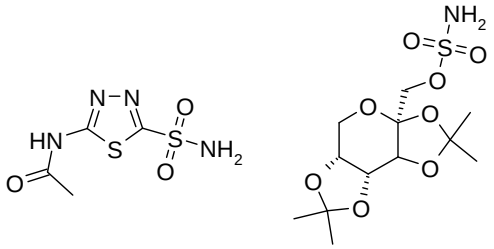

AAZ, 1 **TPM, 2**

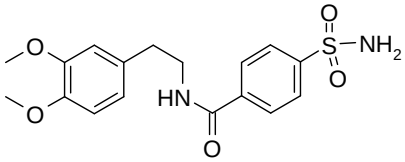

3a

Chart 2.

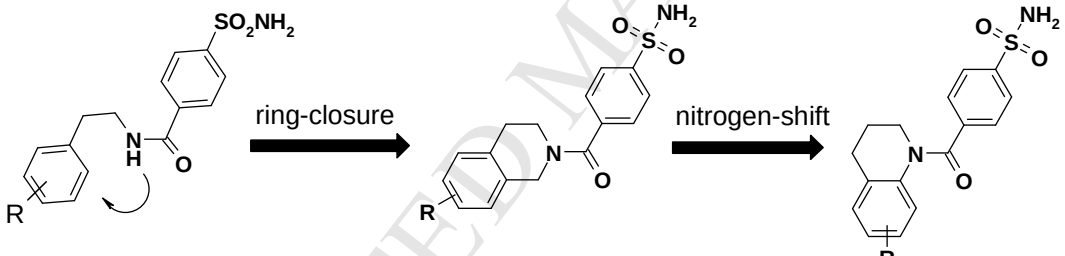

3a, R = 3,4-(OMe)$_2$ **4** **5**

R = H, OMe, OH

List of captions

Chart captions

Chart 1. hCA inhibitors: currently marketed drugs and previously reported benzamide **3a**.

Chart 2. Designed analogues of *N*-(3,4-dimethoxyphenethyl)-4-sulfamoylbenzamide (**3a**).

Figure captions

Figure 1. Interactions of inhibitor **3a** with hCA II in co-crystal structure (PDB code 3V7X).[48] The inhibitor in stick representation has carbon atoms colored turquoise (alternative conformation is shown in lighter shades), other atoms are colored according to standard color coding: oxygen red; nitrogen blue; sulfur yellow. Active site residues involved in the interactions are also shown as sticks with carbon atoms in pink. Polar interactions (direct as well as water-mediated) are represented by dotted lines. Zinc ion and water molecules are represented by grey and red spheres, respectively.

Figure 2. Active site of hCA II coloured by electrostatic potential, the inhibitors are depicted in stick representation. **(A)** hCA II in complex with inhibitor **4a** (orange). (B) comparison of binding pose of the two inhibitors **4b** (yellow) and **4e** (purple).

Figure 3: A. Binding of **5e** into the active site of hCA II**.** Surface of hCA II is coloured by electrostatic potential (blue for positive, red for negative), inhibitor in stick representation has carbon atoms of inhibitor coloured green while other atoms are coloured according to standard color coding: oxygen red; nitrogen blue; sulphur yellow**. B.** Comparison of previously reported inhibitor **3a** in complex with hCA II (PDB code 3V7X)[48] with compound **5e** when co-crystallized with hCA II. The inhibitor in stick representation has carbon atoms colored blue for compound **3a** and green for **5e**. For compound **3a** both alternative conformations are shown, for compound **5e** three alternative conformations are shown; the alternative conformation A with the highest occupancy is marked by black arrow. Residues of hCA II which are in contact with inhibitor are represented by sticks with carbon atoms colored salmon. **C.** Active site of hCA II with inhibitors **5c** and **5e**.Surface of hCA II is coloured red for residues interacting with **5e** only; blue are residues interacting only with **5c** inhibitor and residues interacting with both inhibitors are coloured magenta; the inhibitor **5e** is depicted in line, inhibitor **5c** is in stick representation (carbon atom are coloured black and grey for **5e** and **5c**, respectively).

Figure 4. **A**. Compounds **4b** (yellow), **4e** (blue), and **5c** (pink) docked into hCA VII; the hCA VII hydrophobic cleft is defined by residues Phe131 and Ala135, Pro202, Leu204 (magenta). **B.** Interactions of ligand **4e** with hCA VII; the inhibitor in stick representation has carbon atoms colored in blue marine, other atoms are colored according to standard color coding: oxygen red; nitrogen blue; sulfur yellow. Active site residues involved in the interactions are also shown as sticks with carbon atoms in light grey. Polar interactions are represented by dotted lines. Zinc ion is represented by grey sphere.

Scheme 1

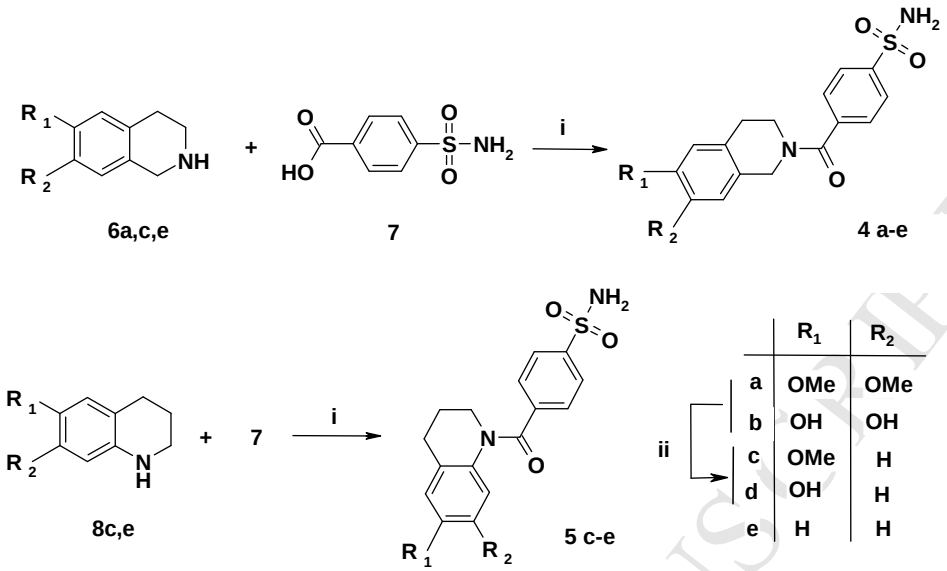

Scheme 1. Reagents and conditions: **i)** HBTU, DMF, TEA, rt, overnight; **ii)** BBr_3(1M in DCM), DCM, rt, overnight.

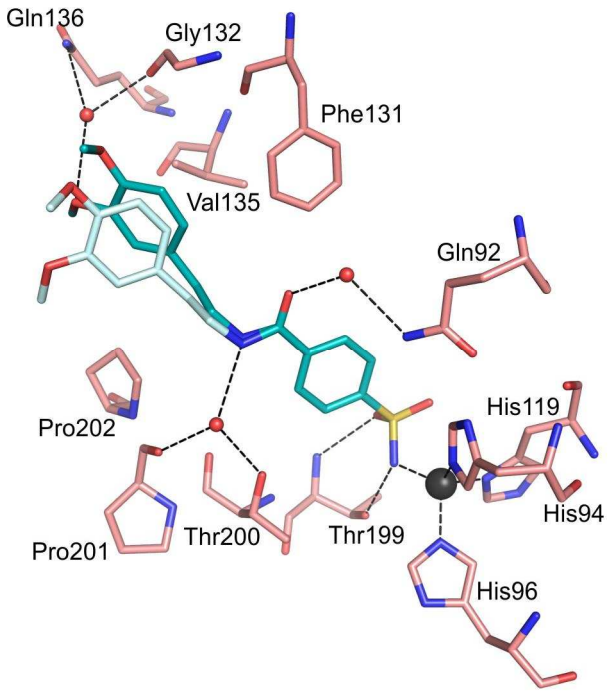

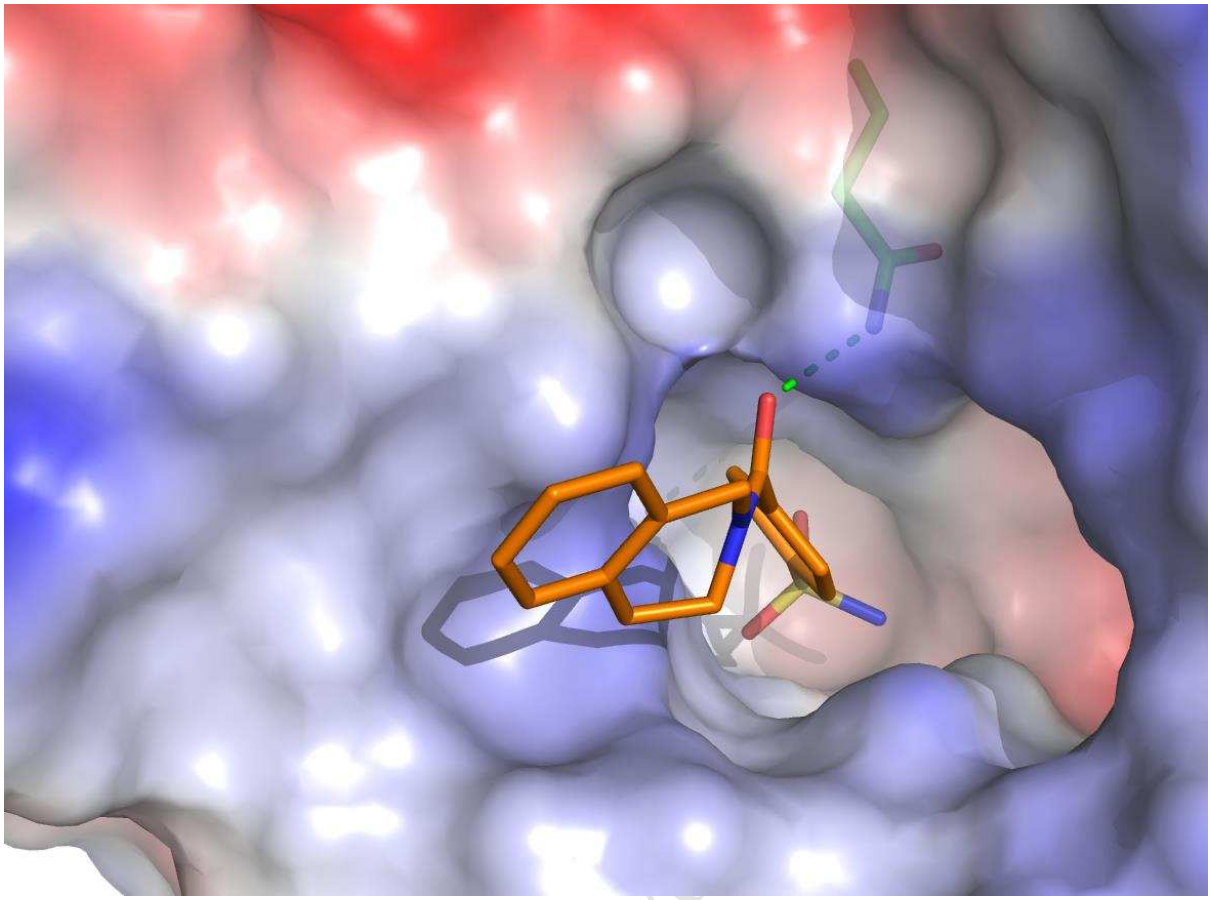

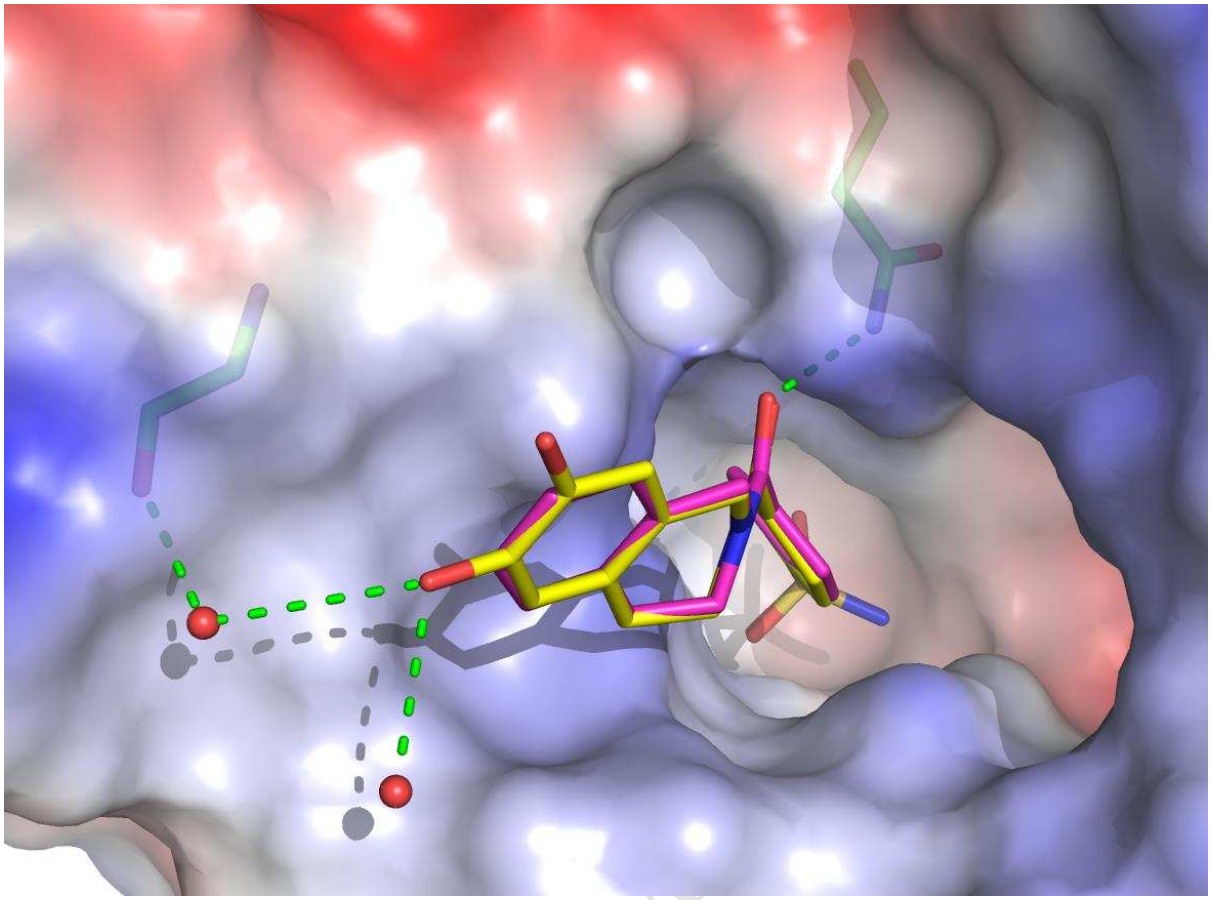

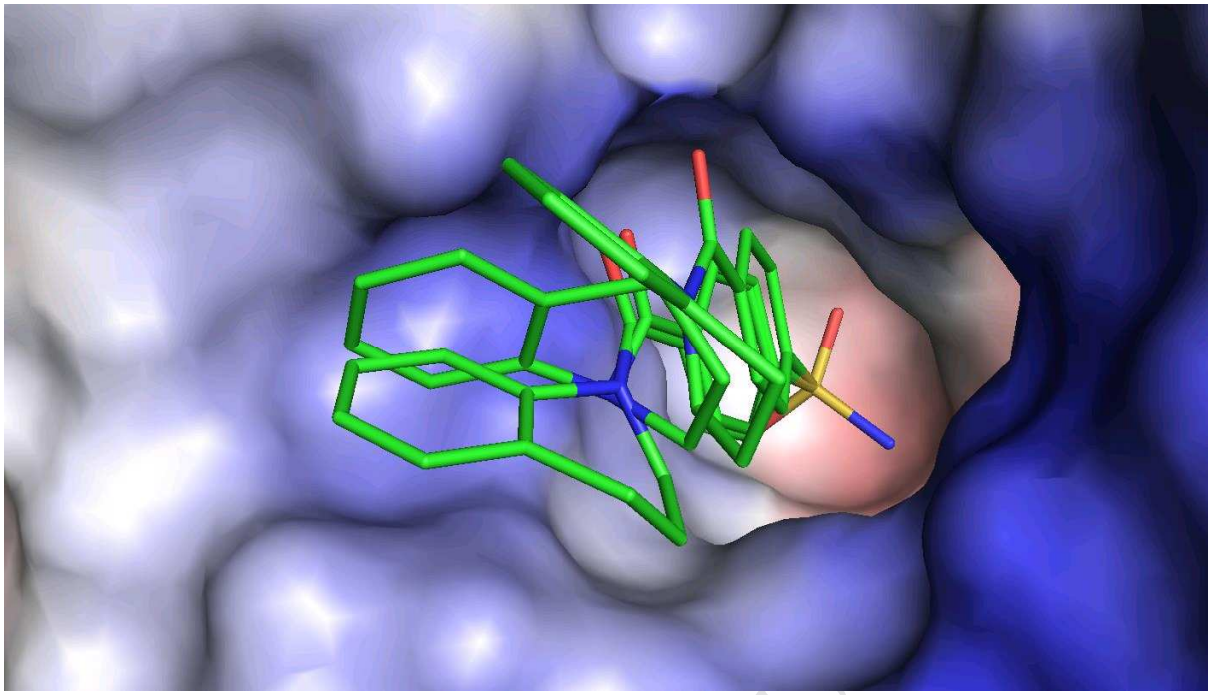

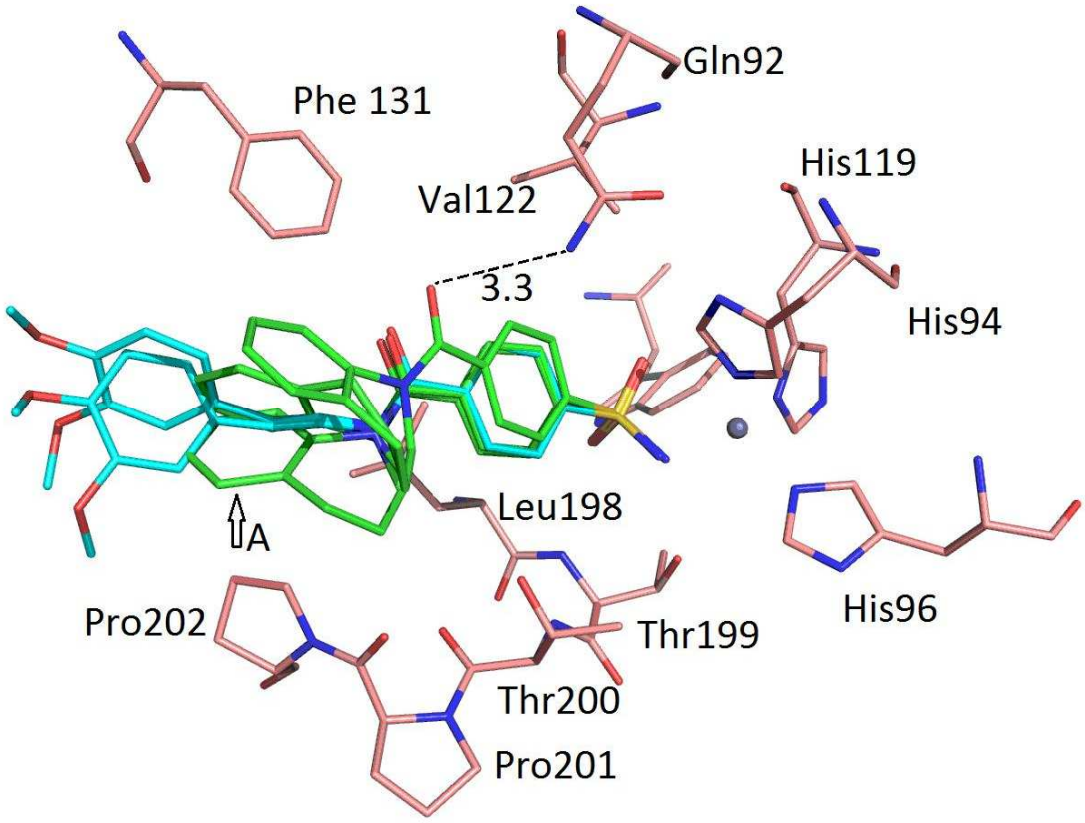

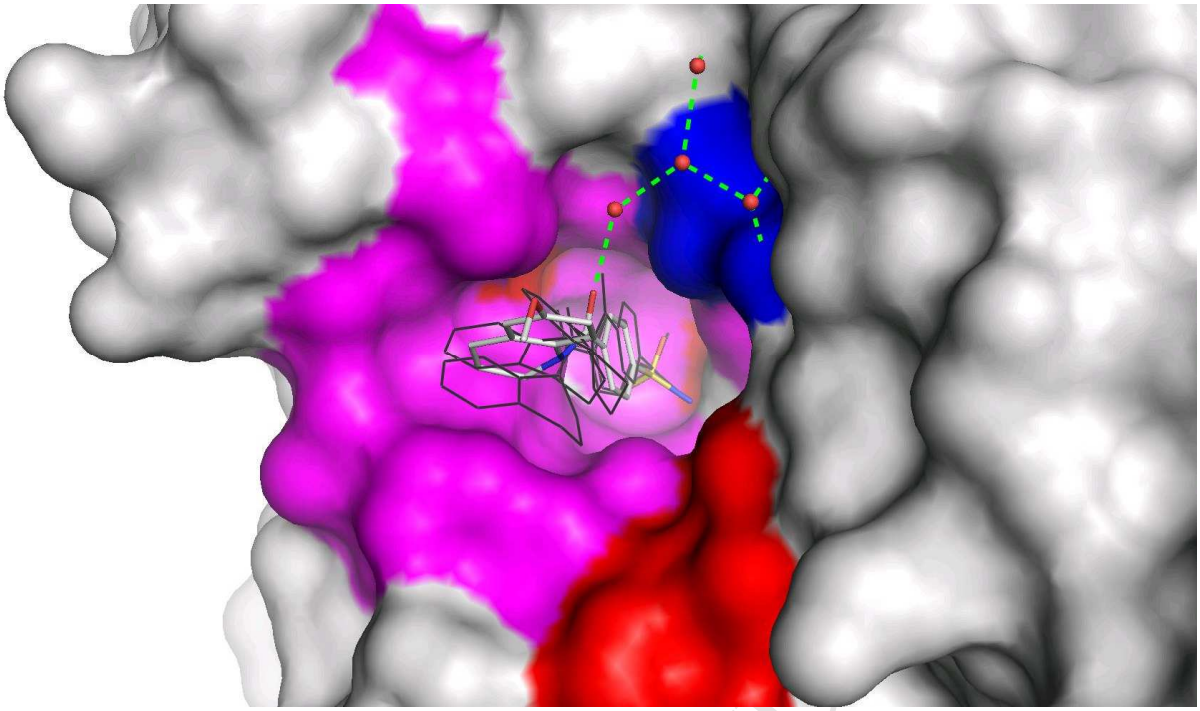

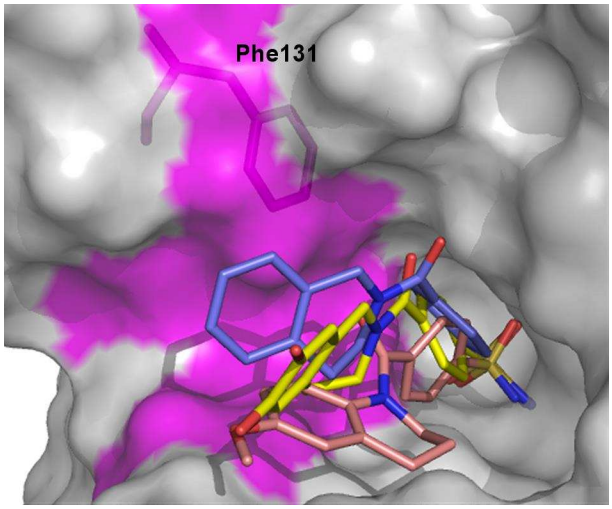

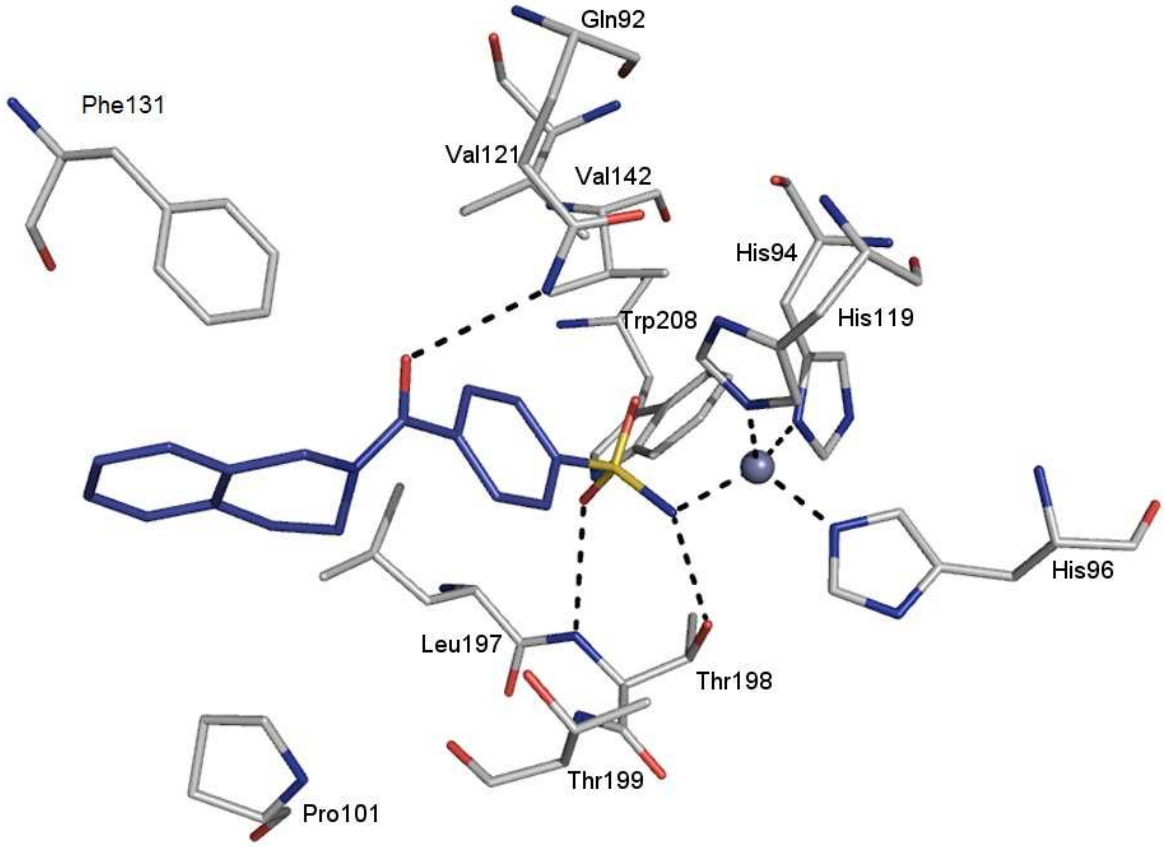

Highlights

- Novel heteroaryl-*N*-carbonylbenzenesulfonamides proved to be potent hCAs inhibitors
- High resolution crystal structures shed light in recognition within hCA II site
- Suitable structural modifications reduce exclusively the hCA VII affinity
- Docking experiments helped us to justify the lack of hCA VII activity

Supplementary material

Carbonic anhydrase inhibitors: Design, synthesis and structural characterization of new heteroaryl-*N*-carbonylbenzenesulfonamides targeting druggable human carbonic anhydrase isoforms

Maria Rosa Buemi, Laura De Luca, Stefania Ferro, Elvira Bruno, Mariangela Ceruso, Claudiu T. Supuran, Klára Pospíšilová, Jiří Brynda, Pavlína Řezáčová, and Rosaria Gitto

^{1}H and ^{13}C NMR Spectra of representative compounds

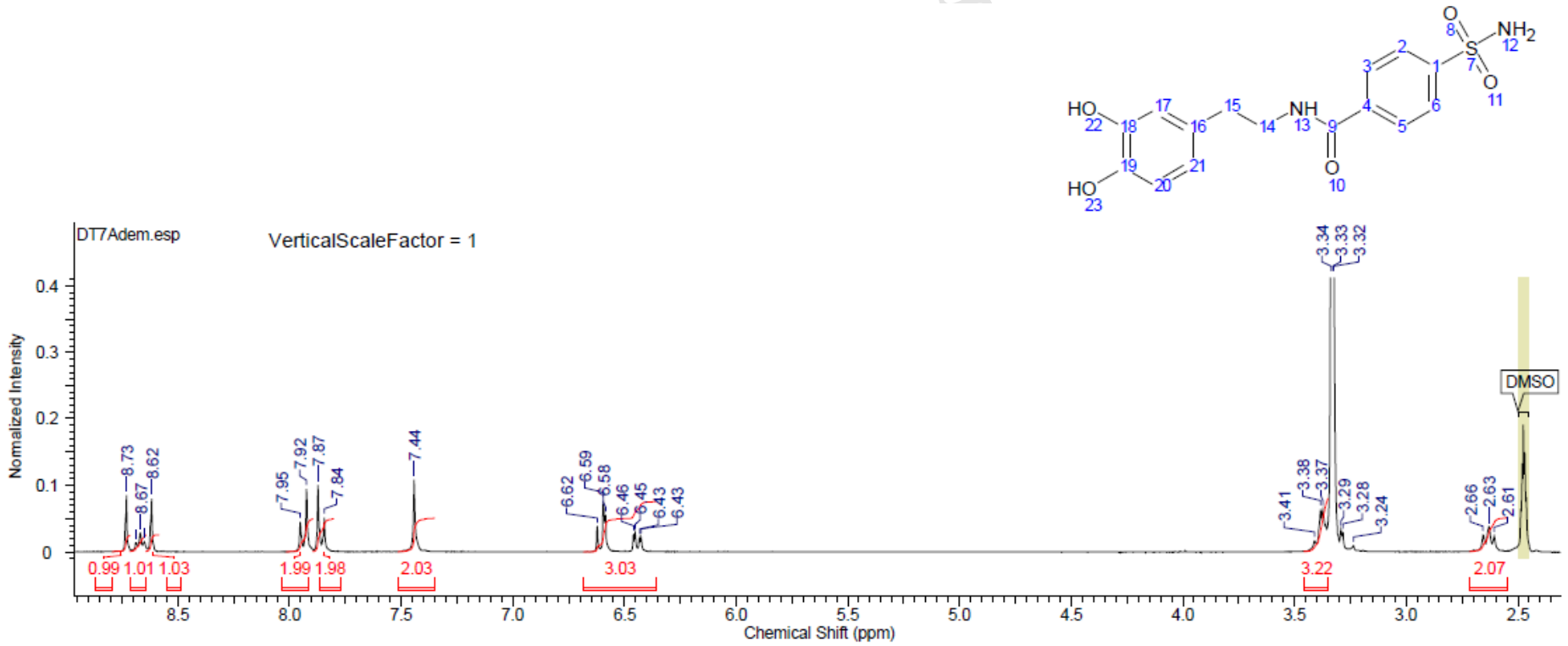

Spectrum 1. ^{1}H NMR Spectrum of compound 3b (300 MHz, DMSO-d_6)

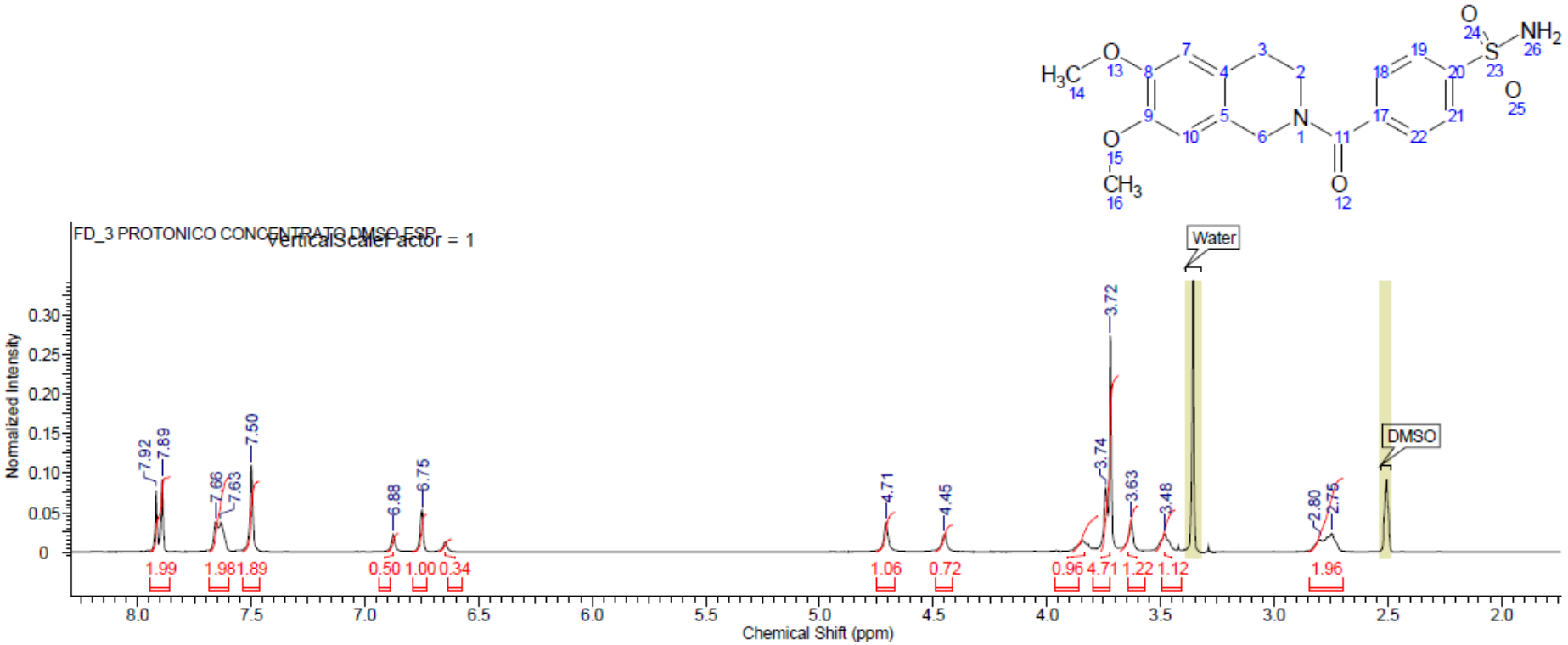

Spectrum 2. ^{1}H NMR Spectrum of compound 4a (300 MHz, DMSO-d_6)

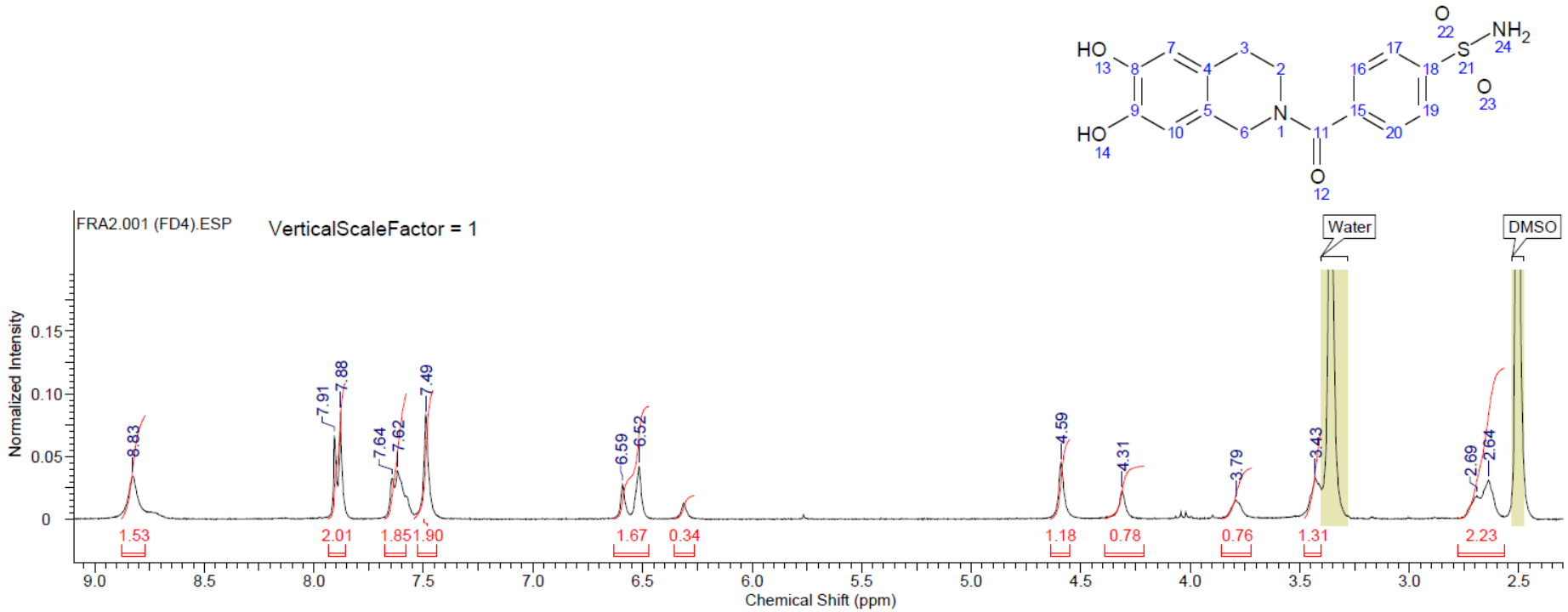

Spectrum 3. ^{1}H NMR Spectrum of compound 4b (300 MHz, DMSO-d_6)

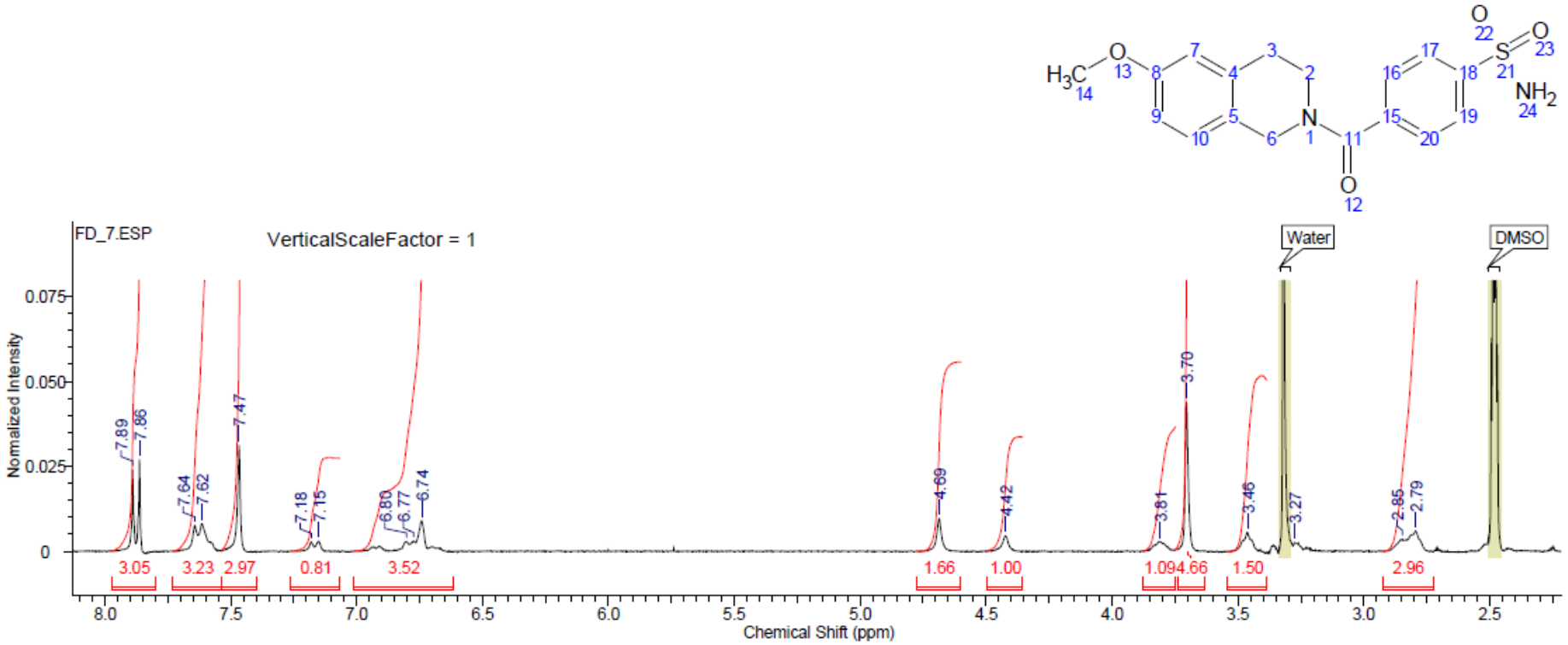

Spectrum 4. ^{1}H NMR Spectrum of compound 4c (300 MHz, DMSO-d_6)

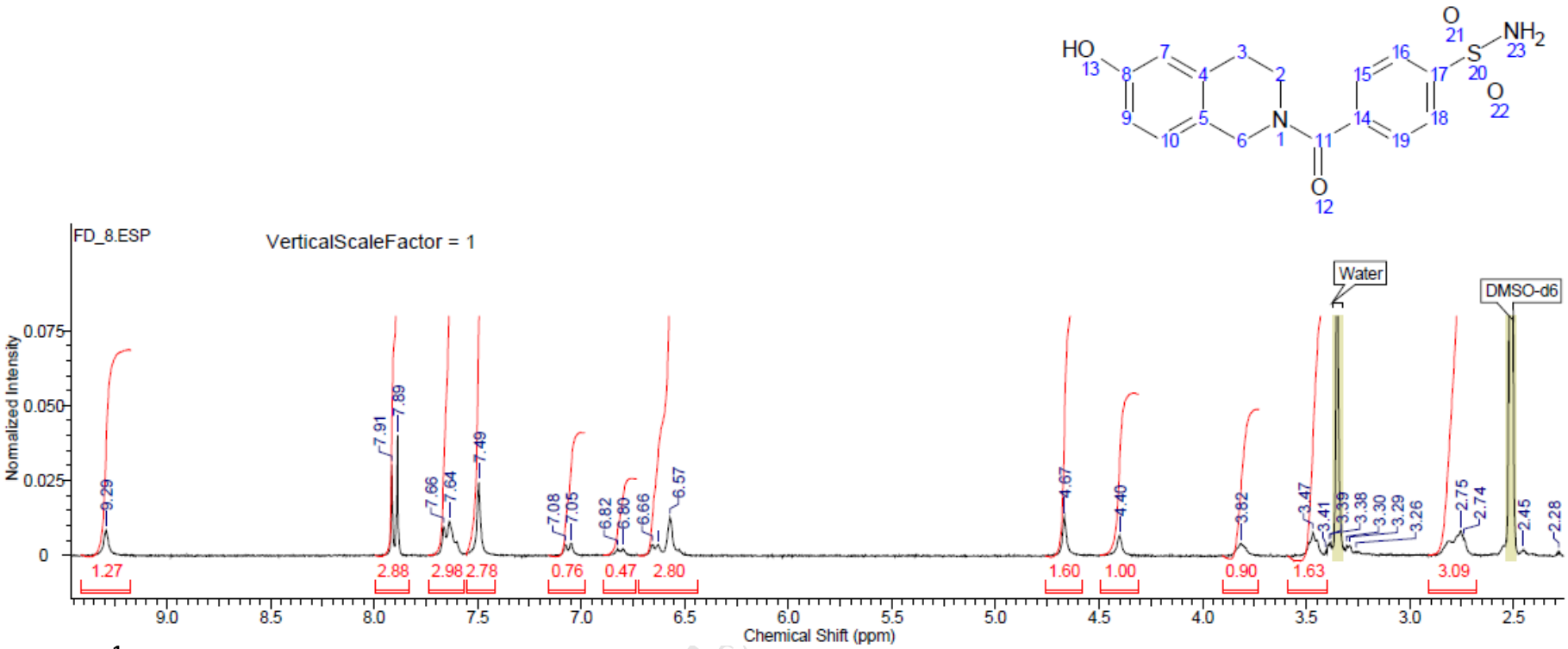

Spectrum 5. ^{1}H NMR Spectrum of compound 4d (300 MHz, DMSO-d_6)

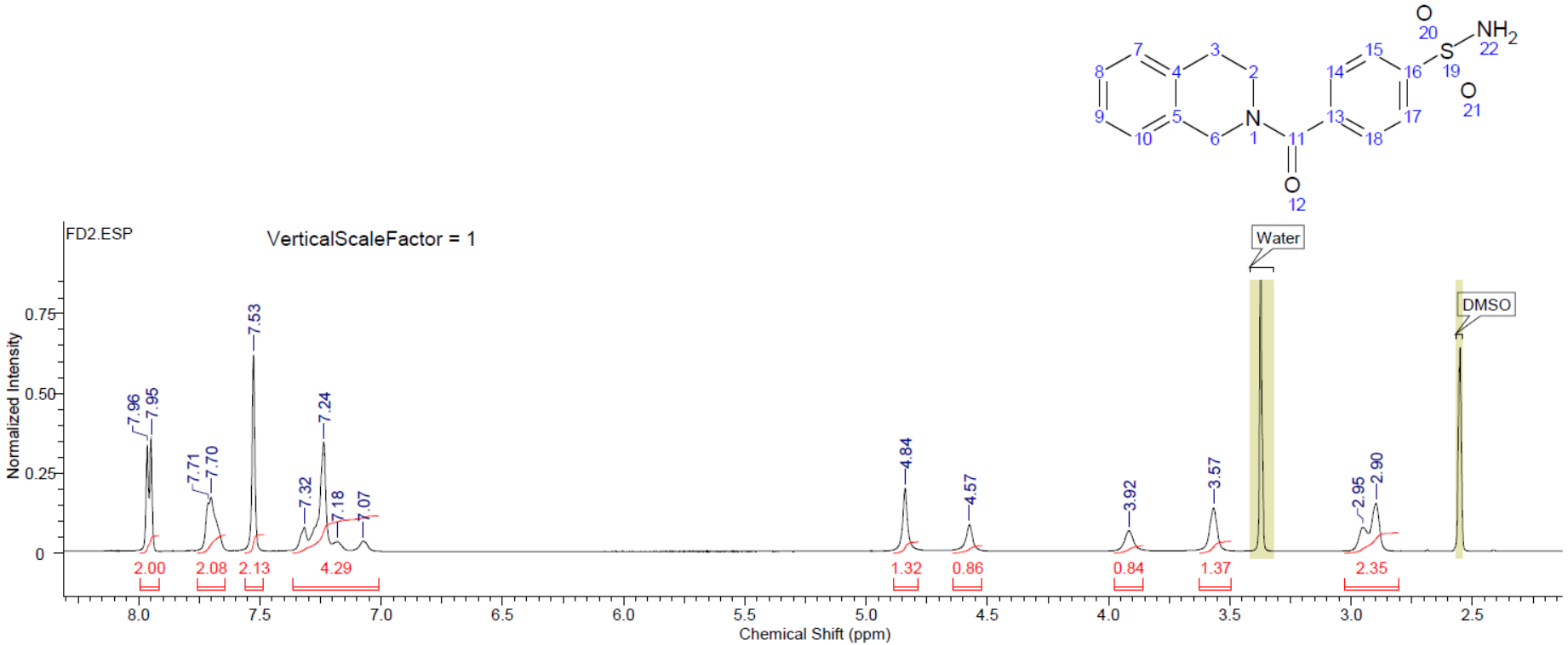

Spectrum 6. ^{1}H NMR Spectrum of compound 4e (300 MHz, DMSO-d_6)

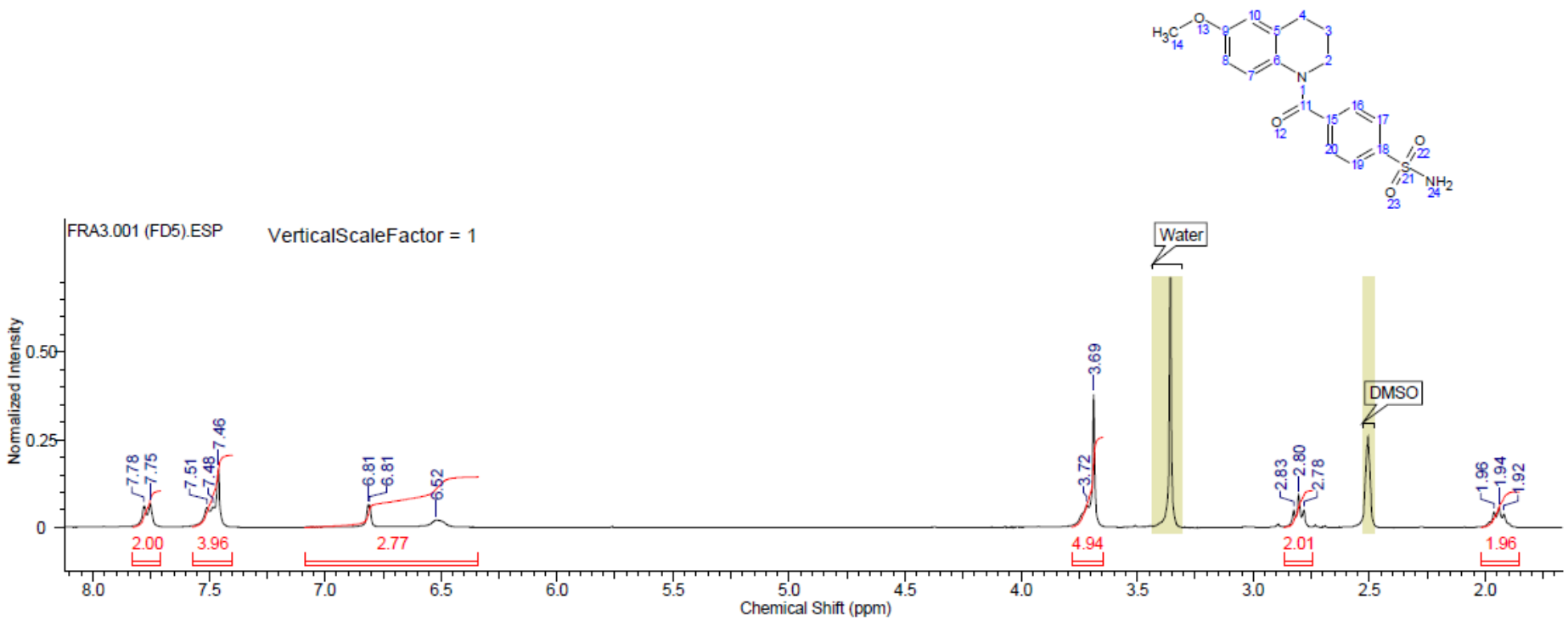

Spectrum 7. ^{1}H NMR Spectrum of compound 5c (300 MHz, DMSO-d_6)

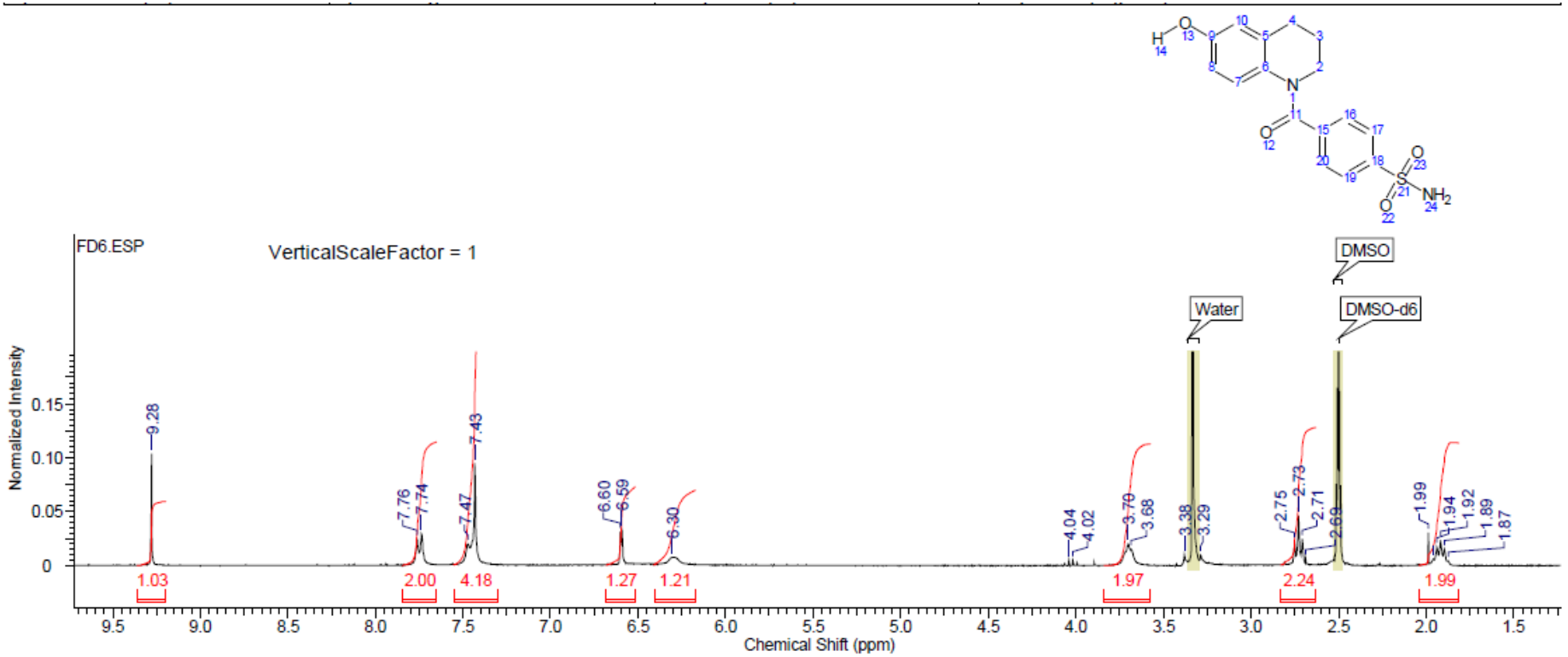

Spectrum 8. ^{1}H NMR Spectrum of compound 5d (300 MHz, DMSO-d_6)

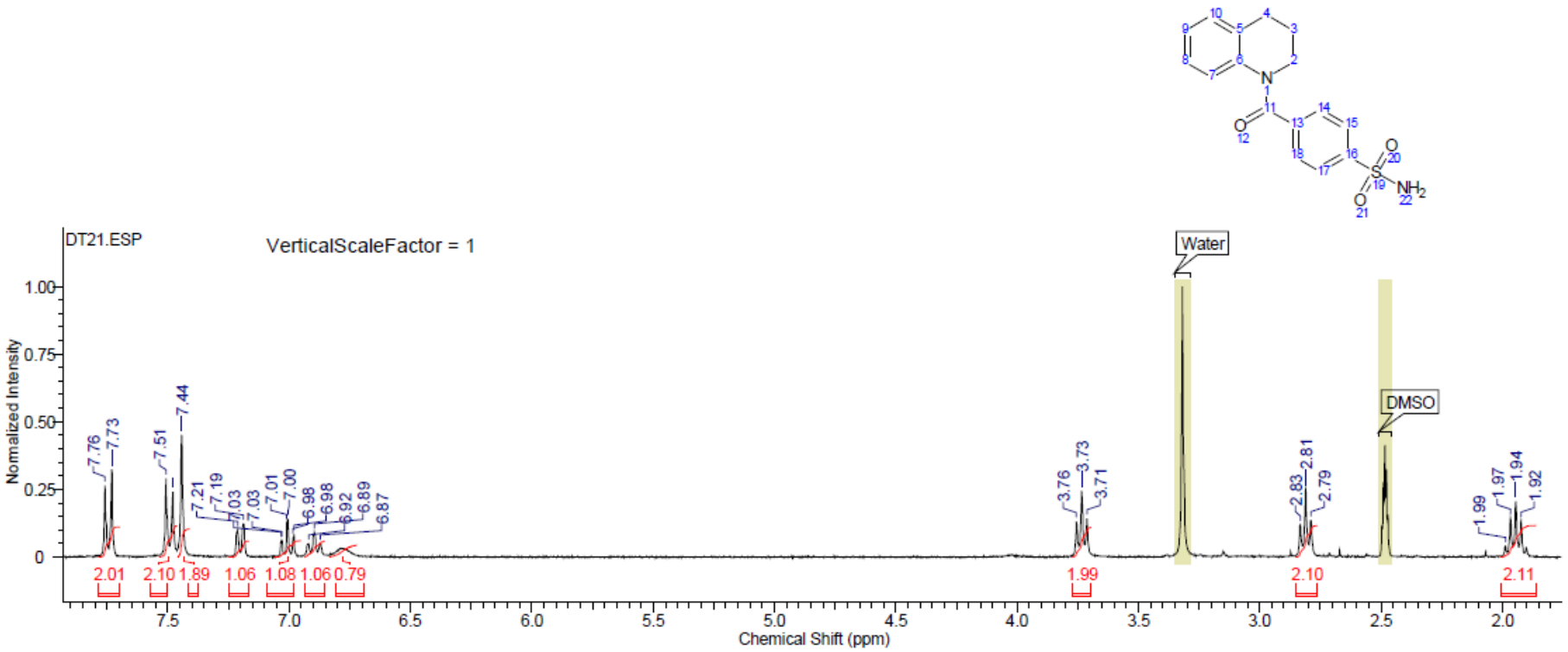

Spectrum 9. ^{1}H NMR Spectrum of compound 5e (300 MHz, DMSO-d_6)

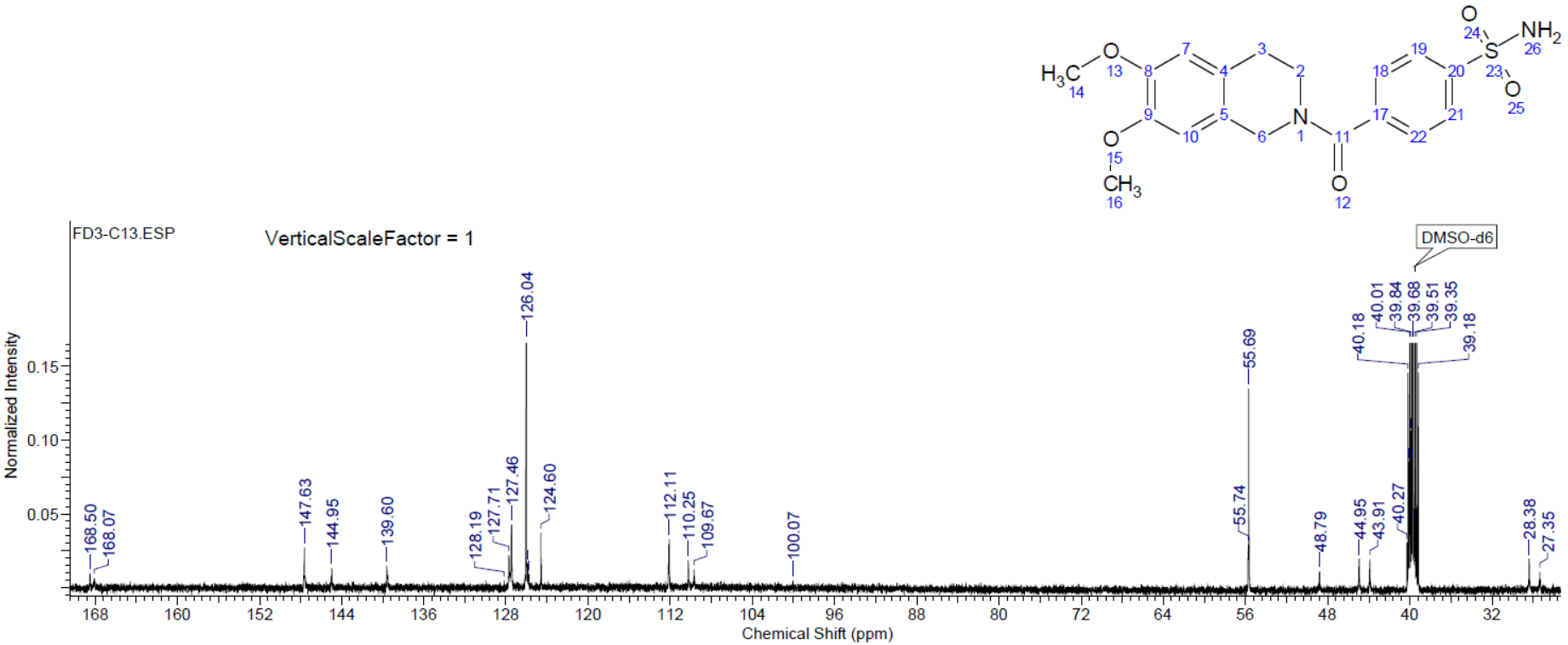

Spectrum 10. ^{13}C NMR Spectrum of compound 4a (125.7 MHz, DMSO-d_6)

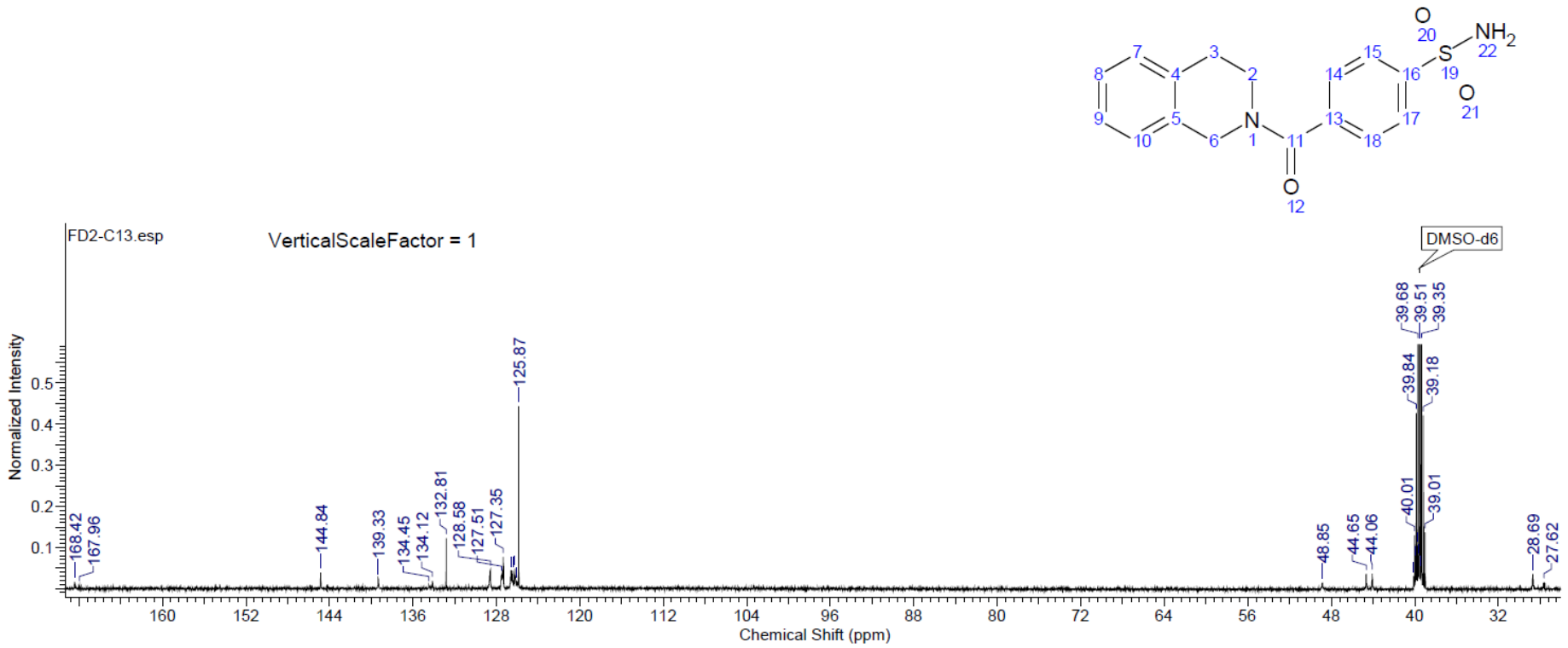

Spectrum 11. ^{13}C NMR Spectrum of compound 4e (125.7 MHz, DMSO-d_6)